Brief communication

Astrocytes modulate neuronal development by S100A6 signaling

Valentina Cinquina[1], Daniela Calvigioni[1,$], Fabiana Piscitelli[2], Erik Keimpema[1], Vincenzo Di Marzo[2,4,5], Alexei Verkhratsky[6,7] and Tibor Harkany[1,8,#]

[1]Department of Molecular Neurosciences, Center for Brain Research, Medical University of Vienna, Vienna, Austria,
[2]Endocannabinoid Research Group, Institute of Biomolecular Chemistry (ICB), National Research Council (CNR), Pozzuoli, Italy,
[4]Institut Universitaire de Cardiologie et de Pneumologie de Québec and Institut sur la Nutrition et les Aliments Fonctionnels, Centre Nutriss, Université Laval, Québec, QC, Canada,
[5]Canada Excellence Research Chair on the Microbiome-Endocannabinoidome Axis in Metabolic Health,
[6]Faculty of Biology, Medicine and Health, The University of Manchester, Manchester, United Kingdom,
[7]Achucarro Centre for Neuroscience, IKERBASQUE, Basque Foundation for Science, Bilbao, Spain,
[8]Department of Neuroscience, Biomedicum 7D, Karolinska Institutet, Solna, Sweden.

[$]*Present address*: Department of Neuroscience, Biomedicum 4B, Karolinska Institutet, Solna, Sweden.

[§]*Correspondence* should be addressed to **Tibor Harkany** (Tibor.Harkany@meduniwien.ac.at).

Abstract

Neuronal morphogenesis relies on intercellular signaling. Astrocytes release metabolites, trophic, and guidance factors to promote neuronal differentiation. In contrast, the mechanisms by which astrocytes could limit and stabilize neuronal connectivity remain less explored. Here, we show cortical astrocytes to express and release S100A6, a Ca^{2+}-binding protein ('calcyclin'). Simultaneously, the majority of cortical neurons express a *bona fide* binding partner for S100A6, calcyclin-binding protein (CaCyBp). In neurons, CaCyBp maintains unfolded protein response, thereby controlling proteostasis. When released, S100A6 inhibits CaCyBp signaling, thus slowing protein turnover, and inhibiting neuritogenesis. S100A6-CaCyBp signaling during gestation and lactation is sensitive to the mother's nutritional status, particularly eicosapentaenoic acid intake. Thus, a member of the S100 protein family acts as an astroglia-derived morphogen, whose action on neurons is modulated by environmental factors.

Key words: calcyclin | calcyclin-binding protein | morphogenesis | cerebral cortex | intercellular communication | UPR pathway.

Reciprocal communication with astrocytes underpins the development, survival, and excitability of neurons. Therein, astrocytes release gliotransmitters (such as canonical neurotransmitters, adenosine/ATP, and trophic factors), neurotransmitter precursors (glutamine, L-serine) and metabolites (chiefly lactate and pyruvate), and also clear excess neurotransmitters and waste products, including potential neurotoxins[1]. During brain development, astrogliogenesis coincides with synaptogenesis[1]. Astrocytes are broadly known to express and release differentiation and survival factors (e.g., *Bdnf, Gdnf,* thrombospondin, hevin/sparcl1) to promote the polarization, morphological differentiation, and synaptogenesis of neuroblasts[1]. In contrast, astrocyte-derived factors that are inhibitory to neuritogenesis, thus acting to balance growth *vs*. synapse selection and stabilization, remain less explored. Considering that major steps of cellular differentiation are regulated by Ca^{2+} signaling (be this the activation of kinases, cytoskeletal instability, directional growth decisions, synaptogenesis)[1], Ca^{2+}-binding and sensor proteins appear particularly important considering that some can even undergo regulated release to support intercellular interactions[2]. In astrocytes, S100β, a Ca^{2+}-binding protein, is best known as one of the 25 members of the S100 protein family[2] because it is constitutively expressed across brain regions[3,4], and associated with inflammation in adults[3,5]. However, if S100 proteins are expressed in astrocytes during brain development and could be assigned to regulate neuronal morphogenesis remains unknown.

Here, we first addressed the expression sites and developmental dynamics of S100 proteins in the mouse brain by re-processing open-label single-cell RNA-seq data on the fetal somatosensory cortex[6]. Fourteen of the S100 proteins were detected from embryonic day (E)10.5 on (**Fig. 1a**). Nine of the proteins gradually increased in expression up to postnatal day (P)4. In contrast, *S100a6* (also termed 'calcyclin') showed a sharp increase between E18.5 and P4, when astrogliogenesis peaks[1,6], and paralleled that of glial fibrillary acidic protein (G*fap*) and aldehyde dehydrogenase 1 family member L1 (*Aldh1l1*), which are prototypic astrocyte markers (**Fig. 1a**). UMAP representation revealed the most pronounced *S100a6* expression in differentiating astrocytes (enriched also in, e.g., *Gfap* and *Apoe*) and oligodendrocytes (*Olig1*, *Olig2,* and *Pfgfra*), and less so in glial progenitors (*Slc1a3* and *Top2a*) (**Fig. 1b**). qPCR and Western blotting validated the presence of *S100a6* mRNA and protein expression, respectively, in late-gestational and neonatal mouse cortices (**Supplementary Fig. 1a-c**). These data suggest that S100A6 might specifically control a hitherto unknown event during brain development, noting that its expression can be maintained in mature astrocytes postnatally[7].

S100A6 binds to calcyclin-binding protein (*Cacybp* or *S100a6bp*), which acts as a bridge to the E3 ubiquitin ligases, *Siah1a/Siah1b*. Thus, S100A6, when released from astrocytes, may regulate protein degradation/turnover in neurons alike in other tissues[8,9], and malignant cells[7]. When testing the availability of *Cacybp* in neurons, we found it ubiquitously expressed at E10.5, with stable levels from E14 to P4 (**Fig. 1a**). *Siah1a* and *Siah1b* were also detected by single-cell RNA-seq (**Fig. 1a**). UMAP assigned *Cacybp* expression to virtually all neuronal lineages in the mouse neocortex (note its lesser expression in astrocytes suggesting cell-autonomous function; **Fig. 1b**). qPCR and Western blotting confirmed stable *Cacybp* mRNA and protein levels, respectively, during development with a robust increase postnatally (**Supplementary Fig. 1b,d,e**). By *in situ* hybridization, we demonstrated the co-localization of *S100a6* and *Gfap* mRNAs, particularly along the walls of the ventricular system (e.g., hippocampal (**Fig. 1c**) and cortical surfaces of the lateral ventricle of mice (**Fig. 1d**)) at E18.5. *Cacybp* expression was confined to cells that co-expressed *Rbofox3* (encoding NeuN). Protein expression was first validated by immunohistochemistry for both S100A6 and CaCyBp in the adult mouse brain (P120), and localized S100A6 in $GFAP^+$ astrocytes (**Fig. 1e**), while CaCyBp marked $NeuN^+$

neurons (**Fig. 1f**). CaCyBp was also seen in the somatodendritic axis of neurons in the cortical plate of human fetuses (2nd trimester; **Fig. 1g**). We then used primary cell cultures enriched in either astrocytes or neurons to show that both the *S100a6*:*Cacybp* mRNA and protein ratios were ~15:1 in astrocytes, whereas ~1:18 in neurons (**Fig. 1h**). Thus, we reveal the mutually exclusive expression of *S100a6* and *Cacybp* in astrocytes *vs*. neurons during corticogenesis and suggest that intercellular S100A6-to-CaCyBp signaling could constitute a novel mode of intercellular communication with S100A6 acting as a *bona fide* gliotransmitter.

For S100A6 be classified as an astrocyte-derived ligand, its expression shall be regulated (e.g., by neurotransmitters and neuromodulators) and undergo activity-dependent release. We tested these properties *in vitro*, under IncuCyte-assisted live-cell imaging to control cell viability, by exposing primary astrocytes to glutamate (100 µM) for up to 6h (**Fig. 2a,b**). Glutamate induced S100A6 accumulation in the culture medium, with a ~5-fold increase by 6h. We propose this to be regulated S100A6 release given the lack of cell death and the parallel (albeit disproportionate) increase in cytosolic S100A6 levels (**Supplementary Fig. 2a**). Next, we asked if S100A6 could bind to CaCyBp by exposing primary cortical neurons to His-tagged recombinant S100A6 ('pulse-chase experiment'). After 30 min, His-S100A6 was detected in neurons by super-resolution microscopy not only at the plasmalemmal surface but also intracellularly (**Fig. 2c**). These data were coherent with subcellular fractionation placing CaCyBp in both the cytosol and, to a lesser extent, membrane fractions (**Fig. 2d; Supplementary Fig. 2b**). Overall, these findings suggest a transcellular action analogous to those of trophic factors and morphogens[10], wherein astroglia could serve as a source of S100A6 regulating neuronal responses by CaCyBp-based ligand recognition[11].

We tested this hypothesis by exposing cortical neurons to recombinant S100A6 (1 µg) for 4 days, which significantly reduced neurite complexity (**Fig. 2e**). This morphogenetic response coincided with reduced CaCyBp protein levels (**Fig. 2f**), which we qualified as a desensitization response. We then knocked down *Cacybp* expression in primary cortical neurons by AAV-mediated shRNA transduction. Attenuated *Cacybp* expression (at 15 days *in vitro*; **Supplementary Fig. 2c,d**) reduced neurite outgrowth relative to mock-transfected controls (**Fig. 2g**). These data identify a role for S100A6 in limiting neuritogenesis through CaCyBp[8,12].

Neuritogenesis relies on the rapid expansion of the cytoskeleton, and enrichment in specific proteins (receptors, transporters) along the neurite axis and in the prospective synapse. Electron microscopy localized CaCyBp in the proximity of the cisternae of the endoplasmic reticulum (ER) of neurons (**Fig. 3a**; **Supplementary Fig. 3a**). This localization suggested that CaCyBp could be poised to affect proteostasis[13] (that is, protein turnover or synthesis at the ER). Indeed, cortical neurons after *Cacybp* knock-down had reduced protein content (*vs*. mock transfected cells; **Fig 3b**). Therefore, we tested the expression of molecular constituents of the ER stress pathway, whose activation increases protein degradation[14] by serving as effectors of the unfolded protein response (UPR) machinery[13]: G-protein coupled receptor 78 (*Gpr78*), cyclic AMP-dependent transcription factor ATF-6 alpha (*Atf6a*), unspliced X-box-binding protein 1 (*Xbp1u*) and spliced X-box-binding protein 1 mRNAs (*Xpi1s)* were all down-regulated (**Fig. 3c**). This suggests the absence of a first phase (acute) cellular response to restore protein homeostasis. Besides live-cell imaging (**Fig. 2b**), we used CCAAT-enhancer-binding protein homologous protein (CHOP)[15] as a surrogate to show that attenuated *Cacybp* expression does not trigger pro-apoptotic signaling (**Fig. 3c**). These results were compatible with a marked increase in tubulin acetylation (**Fig. 3d**), a post-translational mark of long-lived microtubules, suggesting slowed cytoskeletal dynamics[16,17]. These changes were phenocopied by sustained exposure to recombinant

S100A6, which similarly reduced *Cacybp* expression (**Supplementary Fig. 3b-d**). Cumulatively, these data indicate that glia-derived S100A6 could limit neuronal morphogenesis by slowing protein turnover[18].

Next, we sought to address if environmental factors, particularly maternal effectors, that modulate astrogliogenesis could affect S100A6-CaCyBp in the developing brain. We hypothesized that identified eicosapentaenoic acid (EPA), an ω-3 polyunsaturated fatty acid (PUFA), could be one such candidate because it enhances both neurogenesis [19,20] and astrocyte differentiation[21] by being incorporated in the membranes of glial cells[21-23]. However, a biological substrate for EPA is yet unknown. We found that stimulation of cultured astrocytes with EPA (30 μM) for 6h increased both intracellular and extracellular S100A6 levels (**Fig. 3e**) without affecting either astrocyte numbers or viability (**Supplementary Fig. 3e,f**). Thus, we identified S100A6 as a possible released substrate of EPA, at least *in vitro*.

EPA is a key component of 'ω-3 PUFA-enriched' diets in humans, which are preferred during pregnancy. Therefore, we exposed female dams for 8 weeks to a hypercaloric diet enriched in ω-3 PUFAs prior to conception and throughout pregnancy (**Supplementary Table 1**)[24] (EPA enrichment: ~ 5-fold *vs* control diet). We then employed iTRAQ methodology[16] for the unbiased testing of proteins affected by the experimental diet. Amongst the 266 proteins whose levels changed in the fetal cortices at E18.5 (129 *vs*. 137 proteins being up- or down-regulated; **Supplementary Table 2**), we found 18 proteins (7%) of the cluster '*proteasome*' and 48 proteins (18%) of '*translation, ribosome assembly, endoplasmic reticulum*' (**Fig. 3f**), providing coverage of the proteostasis network[25]. Within the '*proteasome*' cluster, CaCyBp was particularly reduced (**Fig. 3g**) and correlated with increased S100A6 levels. Western blotting corroborated the iTRAQ data (**Fig. 3h**). We have also detected reduced total protein content in fetal cortices (**Fig. 3i**) and increased tubulin acetylation (**Fig. 3j**) after gestational exposure to the experimental diet. These data suggest that S100A6-CaCyBp signaling is sensitive to manipulation of dietary PUFA levels during pregnancy, thus affecting cortical architecture[23].

In conclusion, our results describe a novel molecular axis of astrocyte-neuron communication, which is unique in limiting neuronal morphogenesis through the ER/UPS pathway. By using S100A6 as a released ligand, astrocytes can define endpoints of neuronal morphogenesis, particularly neuritogenesis. Therefore, S100A6 is recognized as an astrocyte-specific gliotransmitter, which acts through a signaling cascade centered on the regulation of neuronal proteostasis.

Acknowledgements

We thank J. Mulder and M. Uhlén (Kaarolinska Institutet) for anti-S100A6 and anti-CaCyBp antibodies, G.G. Kovacs (Medical University of Vienna) for human tissues, and S.L. Shirran, C.H. Botting (University of St. Andrews, United Kingdom), M.A. Fuszard (Martin-Luther University, Germany), and P. Poullet (Institut Curie & INSERM U900, France) for iTRAQ proteomics and analysis. This work was supported by the Austrian Science Fund (P 34121-B; E.K.), Swedish Research Council (T.H.); Novo Nordisk Foundation (T.H.); Hjärnfonden (T.H.), the European Research Council (FOODFORLIFE, 2020-AdG-101021016; T.H.), and an intramural research grant of the Medical Neuroscience Cluster of the Medical University of Vienna (2021-1; T.H.).

Author contributions

T.H. conceived the project, V.C., V.D.M., A.V. and T.H. designed experiments; T.H. procured funding, V.C., D.C., F.P., and E.K. performed experiments and analyzed data, V.C. and T.H. wrote the manuscript with input from all co-authors.

Conflict of interest

The authors declare that they have no conflict of interest.

Data availability

iTRAQ data are being deposited in PRIDE with the accession number becoming available by final acceptance.

Supplementary Information is available in the online version of the paper.

Corresponding author statement

Correspondence and requests for materials should be addressed to T.Ha. (tibor.harkany@ki.se or tibor.harkany@meduniwien.ac.at).

Online methods

Animals and ethical approval of *in vivo* studies

Female mice (C57Bl6/J) were housed in groups (5 mice/group) in perplex cages on a 12h/12h light/dark cycle (lights on at 08:00 h) and in a temperature (22 ± 2 °C) and humidity (50 ± 10%)-controlled environment. Food and water were available *ad libitum*. Embryos and tissues were obtained from timed matings with the day of vaginal plug considered as embryonic day (E) 0.5. Group sizes were defined as per conventions in developmental biology[24,26]. Experiments on live animals conformed to the 2010/63/EU European Communities Council Directive and were approved by the Austrian Ministry of Science and Research (66.009/0277-WF/V/3b/2017). Particular effort was directed towards minimizing the number of animals used and their suffering during experiments.

Human tissue, immunohistochemistry

Fetal brains (gestational week (GW) 27; *n* = 3 samples; mixed for sex) were collected at the Neurobiobank of the Institute of Neurology, Medical University of Vienna, Austria. Tissues were obtained and used in compliance with the Declaration of Helsinki and following institutional guidelines approved by the Ethical Committee of the Medical University of Vienna (No. 396/2011). Fetal brain tissue was obtained from spontaneous or medically induced abortions. Fetuses whose cause of death was unrelated to genetic disorders, head injury, neurological diseases, or other known diseases (e.g., infections) were only included. Tissues were kept at 4 °C for 24–48 h due to local regulations before immersion fixation in formalin (10%) on average for 34–37 days before embedding in paraffin. Three-µm tissue sections of formalin fixed, paraffin-embedded tissue blocks were mounted on pre-coated glass slides (StarFrost). Following deparaffinization and rehydration, sections were incubated in a solution of H_2O_2 (3%) and MeOH for 10 min to block endogenous peroxidase activity. After washing with distilled water, sections were pre-incubated in low pH EnVision™ FLEX antigen retrieval solution (PTLink; Dako) at 98 °C for 20 min, exposed to fetal calf serum (10%) for 10 min and subsequently stained with rabbit anti-CaCyBp antibody (**Supplementary Table 3**) at 4 °C for 72 h. The EnVision detection kit (K5007, ready-to-use, DAKO) was used to visualize the horseradish peroxidase/DAB reaction product with H_2O_2 substrate (0.01%). Sections were counterstained with hematoxylin-eosin, dehydrated in an ascending series of ethanol, cleared with xylene and covered with Consil-Mount (Thermo Scientific), and viewed under a light microscope (Nikon Eclipse E400). We did not observe variations in the cellular distribution of CaCyBp across the samples. Therefore, a representative image was included.

Immunohistochemistry, light and electron microscopy

Adult male mice were transcardially perfused with ice-cold 0.1 M PB (20 ml), followed by 4% PFA in PB (100 ml at 3 mL/min flow speed). P120 adult brains were post-fixed in 4% PFA overnight. After equilibrating in 30% sucrose for 48–72 h, coronal serial sections (1-in-6 series) were cryosectioned (Leica CM1850) at a thickness of 50 µm. Free-floating sections were processed as described[27] for either fluorescence microscopy or chromogenic (using 3,3'-diaminobenzidine (DAB) as substrate) electron microscopy.

For fluorescence histochemistry, free-floating sections from *n* = 4 male adult mice were extensively rinsed in PB, and blocked with PB containing 5% normal donkey serum (NDS; Jackson ImmunoResearch), 1% bovine serum albumin (BSA; Sigma), and 0.3% Triton X-100 (Sigma) at 21-24 °C for 2 h to reduce non-specific labeling. Next, sections were incubated with a combination of primary antibodies (**Supplementary Table 3**) diluted in PB also containing 2% NDS, 0.1% BSA and 0.3% Triton X-100 at 4 °C for 72 h. DyLight Fluor 488, 560, or 633-tagged secondary antibodies (1:300; Jackson ImmunoResearch) were used for signal detection. Hoechst 33,342 (Sigma) and 4',6-diamin-2-phenylindol (DAPI, Sigma) were routinely used as nuclear counterstains. After washing in PB and a final rinse in distilled water, free-floating sections were mounted onto fluorescence-free glass slides and coverslipped with Mowiol mounting medium. Fluorescence images were acquired on a Zeiss 880 LSM confocal laser-scanning microscope equipped for maximal signal separation and spectral scanning/unmixing.

Electron microscopy was performed as previously published[28]. Briefly, free-floating sections were washed three times with PB for 5 min each and then treated with 1% H_2O_2 for 10 min to block endogenous peroxidase activity. After rinsing, sections were exposed to a blocking solution (*see above*) at 21-24 °C for 2 h. Sections were then incubated with a rabbit anti-CaCyBp primary antibody (**Supplementary Table 3**) for 72 h. After washing three times, sections were exposed to biotinylated anti-rabbit secondary antibodies (1:200; Jackson ImmunoResearch, 20–22 °C, 2 h), rinsed again in PB, and then exposed to preformed avidin-biotin-peroxidase complexes (1:200, ABC Elite; Vector Laboratories) at 4 °C overnight. Next, biotin-labeled cells were revealed using a peroxidase reaction with DAB alone (5 mg/ml, 0.03% H_2O_2 as substrate, brown reaction product). Sections were subsequently osmificated (1% OsO_4 in PB, 15 min), dehydrated in an ascending ethanol gradient followed by flat embedding in Durcupan (FLUKA, ACM). Ultrathin sections (60 nm) were cut on a Leica ultramicrotome, collected on Formvar-coated single slot grids, and analyzed with a Tecnai 10 electron microscope (FEI; primary magnifications: 6200x; 17500x).

In situ hybridization (HCR-FISH)

Fresh-frozen E18.5 mouse brains were cryosectioned at a thickness of 16 µm and collected on SuperFrost$^+$ glass slides (ThermoFisher). Sections were immersed in 4% PFA solution for 15 min, and dehydrated in an ascending ethanol gradient (50%, 70%, and 100%; 5 min each). The HCR™ RNA-FISH protocol for fresh frozen or fixed frozen tissue section (Molecular Instruments) was used with pre-designed *Cacybp*, *S100a6*, *Rbfox3*, and *Gfap* probes. Samples were imaged on an LSM 880 confocal microscope (Zeiss) at 40× primary magnification.

Neuronal cultures, shRNA knockdown, S100A6 transfection

Cerebral tissues (cortex/hippocampus) of mouse embryos (mixed for sex) were isolated at E18.5 or P0. Cells were mechanically dissociated into single cell suspension by papain digestion (20 U/ml, pH 7.4, 45 min) and plated on poly-D-lysine-coated (PDL; Sigma) 6-well (200,000 cells/well) or 24-well (50,000 cells/well) plates. Cells were maintained in Neurobasal medium (Fisher Scientific) supplemented with B27 (1%; ThermoFisher), GlutaMAX™ (1%; ThermoFisher), and penicillin/streptomycin (1%; Life Technologies). Media were replaced every other day.

For shRNA knockdown of *Cacybp*, P0 cortical neurons (200,000 cells/well) were seeded in 6-well plates, grown for 48 h, then transduced with either 1 µl of adeno-associated virus, serotype 2 (AVV-2) particles (Catalog #: AA02-CS-MSE091282-AVE001-01-200, 6.09 x 10^{12} genome copies/ml, GeneCopoeia™) for shRNA delivery or equal amounts of AVV-2s to deliver scrambled controls (Catalog #: AA02-CS-CSECTR001-AVE001-01-200). Media were replaced with Neurobasal medium (*as above*) free of AAV-2 particles after 48 h, and changed every other day. Cells were then lysed and collected for Western blotting and qPCR after 15 days *in vitro* (DIV). Morphometric analysis of cultured neurons was aided by the ImageJ software and included the length of the primary neurites (µm). Analyses of neuronal morphology were performed on 15 DIV because *Cacybp* mRNA and protein levels were found then significantly reduced in shRNA-exposed samples *vs*. both technical controls and samples treated with scrambled shRNA.

For transient transfection, P0 neurons were plated either at a density of 200,000 cells/well on 6-well plates or at a density of 50,000 cells/well in 24-well plates. After 14 DIV, neurons in 6-well plates were exposed to 1 µg of recombinant His-tagged S100A6 protein (ab108124; Abcam) for 24 h. Cells were then lysed and collected for Western blotting and qPCR. Neurons grown in 24-well plates were exposed to His-tagged S100A6 protein (1 µg) for 30 min on 7 DIV, immersion-fixed in 4% PFA, and exposed to a blocking solution consisting of 10% NDS, 5% BSA, and 0.3% Triton X-100 in 0.1 M phosphate-buffered saline (PBS; pH 7.4) at 21-24 °C for 2 h. Next, neurons were incubated with a combination of anti-CaCyBp and anti-V5 primary antibodies (the latter recognizing the His-tag of the recombinant protein; **Supplementary Table 3**) diluted in PBS also containing 2% NDS, 0.1% BSA and 0.3% Triton X-100 at 4 °C for 24 h. DyLight Fluor 488, 560-tagged secondary antibodies (1:300; Jackson ImmunoResearch) were used for signal detection. Hoechst 33,342 (Sigma) was routinely used as nuclear counterstain. After washing in PBS and a final rinse in distilled water, coverslips were mounted onto fluorescence-free glass slides with Mowiol. Images revealing the subcellular localization of S100A6 were acquired on a Zeiss 880LSM confocal laser scanning microscope with maximal signal separation and spectral scanning/unmixing.

High-throughput neurite tracking

Mouse cerebral cortices were isolated on E18.5. Cells were mechanically dissociated and plated at a density of 20,000 cells/well in PDL-coated 96-well plates for on-line morphometry. After 24 h, E18.5 cultures were exposed to recombinant S100A6 (1 µg) for 4 DIV. Treatment was in quadruplicate and imaged live using an IncuCyte Zoom high-throughput device (Sartorius). Time-lapse images were acquired with 2-h intervals (looped). The growth rate of neurites in each well was obtained by measuring the surface area covered by neurites and expressed as mm/mm^2 surface area. Surface occupancy of the neurons after 4 DIV in culture was computed as the percentage surface area covered by live neurons ('body cluster area'), and considered as a measure of cell survival.

Primary culture of astrocytes, confluence analysis, and S100A6 secretion

Cortices and hippocampi of P7 mice (*n* = 7) were isolated, dissociated into single cell suspension by papain (*as above*), and plated in T75 flasks. Cells were maintained in DMEM (high glucose, 1% GlutaMAX™; ThermoFisher) supplemented with Na-pyruvate (1%; Sigma), fetal bovine serum (FBS; 10%; Sigma) and 1% penicillin/streptomycin. After 7–9 days, T75 flasks were placed on a shaker (180 rpm, 37 °C, overnight) to remove cell debris, neurons, and oligodendrocytes.

For confluence analyses, astrocytes were plated at a density of 7,000 cells/well into 96-well plates. After 24 h, astrocytes were placed in serum-free medium for 24 h, and then treated with glutamate (100 μM; Tocris 0218) and EPA (5, 10 and 30 μM; Cayman #90110) for another 24 h. Before use, glutamate was dissolved in sodium hydroxide, EPA was flushed with N_2, and dissolved in dimethyl sulfoxide. Aliquots were stored in glass amber vials at −20°C until needed. Working concentrations of the EPA stock solution were diluted as appropriated to achieve the necessary final concentration in neuronal media containing BSA as antioxidant. Glutamate and EPA treatments were performed in quadruplicate and imaged live using an IncuCyte Zoom high-throughput imaging device (Sartorius). Time-lapse images were acquired every 2 h. Confluence was determined as above.

To detect S100A6 secretion, astrocytes (1×10^6) were subsequently trypsinated, and seeded in 6-well plates. After 24 h, astrocytes were starved in serum-free medium at 37 °C for 24 h, and then treated with glutamate (100 μM) or EPA (30 μM) for an additional 6 h. Supernatants were collected and concentrated using either Amicon Ultra-4 centrifugal units (3kDa cut-off; Sigma) by centrifugation at 7,500 *g* for 40 min, or Amicon Ultra-0.5 centrifugal units (3kDa cut-off; Sigma) by centrifugation at 14,000 *g* for 30 min. Astrocytes were pelleted, lysed, and used for Western blotting.

MTT assay

The [3-(4,5-dimethylthiazol-2-yl)-2,5-diphenyltetrazolium bromide] (MTT) colorimetric assay was carried out at the end of each IncuCyte run to determine drug effects on the viability of both neurons and astrocytes. MTT (Abcam) was added to each well at a final concentration of 0.5 mg/ml, incubated for 3 h, with the medium then aspirated. One hundred μl of 100% DMSO (Sigma) was then added to each well. After the formazan crystals had dissolved, absorbance was determined spectrophotometrically at 570 nm.

RNA isolation and quantitative PCR

The RNeasy mini kit (Qiagen) was used to extract RNA from mouse cerebral tissues and primary cultures. DNase I was used to eliminate traces of genomic DNA. Total RNA was then reverse transcribed to a cDNA library in a reaction mixture using a high-capacity cDNA reverse transcription kit (Applied Biosystems). The cDNA library was then used for quantitative real-time PCR (CFX-connect, Bio-Rad). Pairs of PCR primers specific for *Cacybp*, *S100a6*, *Gpr78*, *Atf4*, *Atf6a*, *Chop*, *Xbp1u* and *Xbp1s* were designed with Primer Bank and the NCBI Primer Blast software (**Supplementary Table 4**). Quantitative analysis of gene expression was performed with SYBR Green Master Mix Kit (Life Technologies). Expression levels were normalized to glyceraldehyde-3-phosphate dehydrogenase (*Gapdh*), a housekeeping gene, for every sample in parallel assays ($n \geq 3$ biological replicates/group).

Total protein determination and subcellular fractionation

Total protein was extracted from cerebral tissues and primary cultures by using a modified radioimmunoprecipitation assay buffer containing 5 mM NaF (Sigma), 5 mM Na_3VO_4 (Sigma), 0.1% N-octyl-β-d-glucopyranoside (Sigma), and a cocktail of protease inhibitors (Complete™, Roche). Samples were homogenized by sonication, and protein lysates were pelleted at 10,000 *rpm* at 4 °C for 10 min. To fractionate membranes

368 and cytoplasm, samples were homogenized by sonication in 25 mM Hepes (pH 7.5; Sigma), 1 mM EDTA
369 (Sigma), 6 mM $MgCl_2$ (Sigma), 1 mM dithiothreitol (DTT; Sigma) and a cocktail of protease inhibitors and
370 centrifuged at 700 *g* at 4 °C for 5 min. The supernatant was centrifuged twice at 14,400 *g* at 4 °C for 30 min
371 then used as cytoplasmic lysate. The pellet was reconstituted as the membrane fraction. Protein concen-
372 trations were determined by Bradford's colorimetric method[29]. The GluA2 subunit of the AMPA receptor
373 (GluA2), vesicle-associated membrane protein 2 (VAMP2), synaptosomal-associated protein 25 (SNAP25),
374 and the mitochondrial import receptor subunit homolog TOM20 were used to control enrichment of the
375 pan-membrane fraction (**Supplementary Table 3**).
376
377
378 **Quantitative Western blotting with total protein normalization**
379 Total protein labeling was initiated by carbocyanine (Cy)5 dye reagent (GE Healthcare) that had been pre-
380 diluted (1:10) in ultrapure water. Samples were mixed and incubated at 21-24 °C for 5 min. The labeling
381 reaction was terminated by adding Amersham WB loading buffer (GE Healthcare; 20 µl/sample) containing
382 40 µM DTT. Equal amounts of the samples (20 µg/40 µl) were then boiled at 95 °C for 3 min, and then
383 loaded onto an Amersham WB gel card (13.5%). Electrophoresis (600 V, 42 min) and protein transfer onto
384 PVDF membranes (100 V, 30 min) were at default settings in an integrated Amersham WB system (GE
385 Healthcare) for quantitative SDS-PAGE and Western blotting of proteins with fluorescence detection. After
386 blocking, membranes were incubated with primary antibodies overnight (**Supplementary Table 3**). Anti-
387 body binding was detected by using species-specific Cy3-labeled secondary antibodies (1:1,000; GE
388 Healthcare). Membranes were dried before scanning at 560 nm (Cy3) and 630 nm (Cy5) excitation. Auto-
389 mated image analysis was performed with the Amersham WB evaluation software with linear image opti-
390 mization, if necessary.
391
392
393 **Prenatal exposure to an experimental diet**
394 Female C57Bl6/J animals at 6 weeks of age were randomly assigned to either a hypercaloric diet enriched
395 ~70-fold in ω-3 PUFAs or a standard diet (**Supplementary Table 1**). Prospective dams consumed the exper-
396 imental diet for 8 weeks prior to conception. Diets were from Special Diet Services (United Kingdom) and
397 quality controlled by mass-spectrometry. The effect of maternal nutrition on fetal brain development was
398 evaluated at E18.5[24]. Embryos were collected from $n \geq 5$ different pregnancies to keep the number of inde-
399 pendent observations sufficient for statistical analyses, sexed if appropriate, and used for histochemistry,
400 proteomics, and molecular biology. The use of specific or mixed genders for particular experiments was
401 specified throughout. Embryos were collected by Cesarean sections from mothers terminally anesthetized
402 by isoflurane (5%, 1 L/min flow rate), weighed, and decapitated with their heads either immersed in 4%
403 PFA in 0.1 M PB (pH 7.4) overnight or snap-frozen in liquid N_2 and stored at -80° C [26,30].
404
405
406 **iTRAQ proteomics**
407 Single cortical hemispheres (*n* = 6/group, mixed and balanced for sex from independent pregnancies) were
408 obtained from E18.5 fetuses. Contralateral hemispheres were snap frozen for target validation by real-time
409 PCR and/or Western blotting. Proteins were extracted by homogenization in lysis buffer (pH 10.0) of tri-
410 ethylammonium bicarbonate (25 mM, Sigma), Na_2CO_3 (20 mM, Sigma) in the presence of protease inhibi-
411 tors (Complete™, EDTA-free Protease Inhibitor Cocktail; Sigma). Protein concentrations were determined

by the bicinchoninic acid assay (ThermoFisher). After quantification, proteins were precipitated in 6 volumes of ice-cold acetone. One hundred µg of proteins per sample were used for isobaric tagging for relative and absolute quantitation (iTRAQ) in an 8-plex layout per the manufacturer's instructions (ABSciex). In brief, proteins were denatured, reduced, alkylated, trypsin digested (Promega), individually labeled with appropriate iTRAQ tags, pooled, concentrated, re-suspended in 1.4 ml loading buffer (10 mM KH2PO4, pH 3.0 in 25% acetonitrile) and sonicated.

Peptides were separated by cation exchange chromatography on a PolySulfoethyl A column (PolyLC) over 30 min with a KCl gradient increasing up to 0.5 M, with 0.5 ml fractions collected. Fifteen fractions across the elution profile of similar peptide concentration were generated and concentrated (SpeedVac). Fractions were re-suspended in 0.1% trifluoroacetic acid (TFA) and desalted on C18 spin columns (PepClean C18, Thermo Scientific). Half of each fraction was then injected on an Acclaim PepMap 100 C18 trap and an Acclaim PepMap RSLC C18 column (Thermo Scientific), using a nanoLC Ultra 2D plus loading pump and nanoLC as-2 autosampler (Eksigent). The peptides were loaded onto the trap in a mixture of 98% water, 2% acetonitrile and 0.05% TFA, washed for 20 min to waste before switching in line with the column, and were then eluted with a gradient of increasing acetonitrile, containing 0.1% formic acid (2-20% acetonitrile in 90 min, 20-40% in a further 30 min, followed by 98% acetonitrile to clean the column before re-equilibration to 2% acetonitrile). The eluate was sprayed into a TripleTOF 5600 electrospray tandem mass spectrometer (ABSciex) and analyzed in Information Dependent Acquisition (IDA) mode, performing 120 ms of MS followed by 80 ms MSMS analyses on the 20 most intense peaks seen by MS, with the 'Adjust Collision Energy when using iTRAQ reagent' box ticked in the method. The data files were processed by ProteinPilot 4.5 (Sciex) using the Paragon algorithm, searching against the SwissProt database (March 2013 edition). The following settings were selected: sample type: iTRAQ 8-plex (peptide labelled), cysteine alkylation: MMTS, digestion: trypsin, instrument: TripleTOF 5600, species: mouse, ID focus: biological modifications and amino acid substitutions and search effort: thorough. Results files were exported into Microsoft Excel, with statistical analysis in SPSS v. 21.

Statistical analysis and figure design

The number of independent samples is indicated in either the individual figure panels or their associated legends. Likewise, the number of animals is given where relevant. All values represent the means ± s.d. of independent experiments. Biological variation among the samples was similar throughout. Statistical significance was determined by Student's *t*-test (for independent groups, two-tailed) or one-way analysis of variance (ANOVA) followed by Bonferroni's *post-hoc* correction (for multiple groups). Statistical analysis was performed in Prism 8.0 (GraphPad Software Inc.). Statistical significance was indicated as follows: $*p < 0.05$, $**p < 0.01$, $***\ p < 0.001$, $****\ p < 0.0001$. Multi-panel images were assembled in CorelDraw 2022 using linear color, brightness or contrast enhancement to increase visual clarity, if necessary.

References

1 Verkhratsky, A. & Butt, A. *Neuroglia: function and pathology*. (Elsevier, 2023).

2 Moore, B. W. A soluble protein characteristic of the nervous system. *Biochem Biophys Res Commun* **19**, 739-744, doi:10.1016/0006-291x(65)90320-7 (1965).

3 Leclerc, E., Sturchler, E. & Vetter, S. W. The S100B/RAGE Axis in Alzheimer's Disease. *Cardiovasc Psychiatry Neurol* **2010**, 539581, doi:10.1155/2010/539581 (2010).

4 Savchenko, V. L., McKanna, J. A., Nikonenko, I. R. & Skibo, G. G. Microglia and astrocytes in the adult rat brain: comparative immunocytochemical analysis demonstrates the efficacy of lipocortin 1 immunoreactivity. *Neuroscience* **96**, 195-203, doi:10.1016/s0306-4522(99)00538-2 (2000).

5 Xia, C., Braunstein, Z., Toomey, A. C., Zhong, J. & Rao, X. S100 Proteins As an Important Regulator of Macrophage Inflammation. *Front Immunol* **8**, 1908, doi:10.3389/fimmu.2017.01908 (2017).

6 Di Bella, D. J. *et al.* Molecular logic of cellular diversification in the mouse cerebral cortex. *Nature* **595**, 554-559, doi:10.1038/s41586-021-03670-5 (2021).

7 Yamashita, N., Ilg, E. C., Schafer, B. W., Heizmann, C. W. & Kosaka, T. Distribution of a specific calcium-binding protein of the S100 protein family, S100A6 (calcyclin), in subpopulations of neurons and glial cells of the adult rat nervous system. *J Comp Neurol* **404**, 235-257 (1999).

8 Schneider, G. & Filipek, A. S100A6 binding protein and Siah-1 interacting protein (CacyBP/SIP): spotlight on properties and cellular function. *Amino Acids* **41**, 773-780, doi:10.1007/s00726-010-0498-2 (2011).

9 Filipek, A., Puzianowska, M., Cieslak, B. & Kuznicki, J. Calcyclin--Ca(2+)-binding protein homologous to glial S-100 beta is present in neurones. *Neuroreport* **4**, 383-386, doi:10.1097/00001756-199304000-00010 (1993).

10 Allaman, I., Belanger, M. & Magistretti, P. J. Astrocyte-neuron metabolic relationships: for better and for worse. *Trends Neurosci* **34**, 76-87, doi:10.1016/j.tins.2010.12.001 (2011).

11 Wasik, U., Kadziolka, B., Kilanczyk, E. & Filipek, A. Influence of S100A6 on CacyBP/SIP Phosphorylation and Elk-1 Transcriptional Activity in Neuroblastoma NB2a Cells. *J Cell Biochem* **117**, 126-131, doi:10.1002/jcb.25257 (2016).

12 Donato, R., Sorci, G. & Giambanco, I. S100A6 protein: functional roles. *Cell Mol Life Sci* **74**, 2749-2760, doi:10.1007/s00018-017-2526-9 (2017).

13 Karagoz, G. E., Acosta-Alvear, D. & Walter, P. The Unfolded Protein Response: Detecting and Responding to Fluctuations in the Protein-Folding Capacity of the Endoplasmic Reticulum. *Cold Spring Harb Perspect Biol* **11**, doi:10.1101/cshperspect.a033886 (2019).

14 Almanza, A. *et al.* Endoplasmic reticulum stress signalling - from basic mechanisms to clinical applications. *FEBS J* **286**, 241-278, doi:10.1111/febs.14608 (2019).

15 Marciniak, S. J. *et al.* CHOP induces death by promoting protein synthesis and oxidation in the stressed endoplasmic reticulum. *Genes Dev* **18**, 3066-3077, doi:10.1101/gad.1250704 (2004).

16 Tortoriello, G. *et al.* Miswiring the brain: Delta9-tetrahydrocannabinol disrupts cortical development by inducing an SCG10/stathmin-2 degradation pathway. *EMBO J* **33**, 668-685, doi:10.1002/embj.201386035 (2014).

17 Maruta, H., Greer, K. & Rosenbaum, J. L. The acetylation of alpha-tubulin and its relationship to the assembly and disassembly of microtubules. *J Cell Biol* **103**, 571-579, doi:10.1083/jcb.103.2.571 (1986).

18 Laguesse, S. *et al.* A Dynamic Unfolded Protein Response Contributes to the Control of Cortical Neurogenesis. *Dev Cell* **35**, 553-567, doi:10.1016/j.devcel.2015.11.005 (2015).

19 Borsini, A., Stangl, D., Jeffries, A. R., Pariante, C. M. & Thuret, S. The role of omega-3 fatty acids in preventing glucocorticoid-induced reduction in human hippocampal neurogenesis and increase in apoptosis. *Transl Psychiatry* **10**, 219, doi:10.1038/s41398-020-00908-0 (2020).

20 Borsini, A. *et al.* Omega-3 polyunsaturated fatty acids protect against inflammation through production of LOX and CYP450 lipid mediators: relevance for major depression and for human hippocampal neurogenesis. *Mol Psychiatry* **26**, 6773-6788, doi:10.1038/s41380-021-01160-8 (2021).

21 Yu, J. Z., Wang, J., Sheridan, S. D., Perlis, R. H. & Rasenick, M. M. N-3 polyunsaturated fatty acids promote astrocyte differentiation and neurotrophin production independent of cAMP in patient-derived neural stem cells. *Mol Psychiatry* **26**, 4605-4615, doi:10.1038/s41380-020-0786-5 (2021).

22 Laye, S., Nadjar, A., Joffre, C. & Bazinet, R. P. Anti-Inflammatory Effects of Omega-3 Fatty Acids in the Brain: Physiological Mechanisms and Relevance to Pharmacology. *Pharmacological reviews* **70**, 12-38, doi:10.1124/pr.117.014092 (2018).

23 Madore, C. *et al.* Essential omega-3 fatty acids tune microglial phagocytosis of synaptic elements in the mouse developing brain. *Nat Commun* **11**, 6133, doi:10.1038/s41467-020-19861-z (2020).

24 Cinquina, V. *et al.* Life-long epigenetic programming of cortical architecture by maternal 'Western' diet during pregnancy. *Molecular psychiatry* **25**, 22-36, doi:10.1038/s41380-019-0580-4 (2020).

25 Hipp, M. S., Kasturi, P. & Hartl, F. U. The proteostasis network and its decline in ageing. *Nat Rev Mol Cell Biol* **20**, 421-435, doi:10.1038/s41580-019-0101-y (2019).

References to Online Methods

26 Calvigioni, D. *et al.* Functional Differentiation of Cholecystokinin-Containing Interneurons Destined for the Cerebral Cortex. *Cereb Cortex* **27**, 2453-2468, doi:10.1093/cercor/bhw094 (2017).

27 Berghuis, P. *et al.* Hardwiring the brain: endocannabinoids shape neuronal connectivity. *Science* **316**, 1212-1216, doi:10.1126/science.1137406 (2007).

28 Malenczyk, K. *et al.* A TRPV1-to-secretagogin regulatory axis controls pancreatic beta-cell survival by modulating protein turnover. *EMBO J* **36**, 2107-2125, doi:10.15252/embj.201695347 (2017).

29 Bradford, M. M. A rapid and sensitive method for the quantitation of microgram quantities of protein utilizing the principle of protein-dye binding. *Analytical biochemistry* **72**, 248-254 (1976).

30 Keimpema, E. *et al.* Differential subcellular recruitment of monoacylglycerol lipase generates spatial specificity of 2-arachidonoyl glycerol signaling during axonal pathfinding. *J Neurosci* **30**, 13992-14007, doi:10.1523/JNEUROSCI.2126-10.2010 (2010).

Legends to Figures, Supplementary Figures and Supplementary Tables

Figure 1. S100A6-to-CaCyBp signaling is an intercellular signaling module. a. Single-cell RNA-seq-based developmental expression patterns for S100 proteins, classical astrocyte markers (*Gfap*, *Aldh1l1*), calcyclin-binding protein (*Cacybp*) and Siah1a/b E3 ubiquitin ligases in the mouse neocortex from embryonic (E) to postnatal (P) days as indicated. **b.** Cell type assignment for *S100a6* and *Cacybp* by UMAP. **c,d.** Mutually exclusive expression of *S100a6* and *Cacybp* with *Gfap* and *Rbfox3* (NeuN) transcripts, respectively, in the fetal mouse brain. Insets are high-resolution images of the areas marked by open rectangles. *Scale bars* = 60 μm and 12 μm (*insets*). *Abbreviations*: CP, cortical plate; LV, lateral ventricle; SVZ, subventricular zone; VZ, ventricular zone. **e.** S100A6 and GFAP co-localization in the adult mouse brain. **f**. Likewise, CaCyBp and NeuN co-existence in the neocortex in adulthood. Open rectangles pinpoint the location of high-power insets. *Scale bars* = 100 μm and 8 μm. *Abbreviations*: Ctx, cortex; int, internal capsule. **g.** CaCyBp localization to the somatodendritic axis of cortical neurons in a human fetus at gestational week (GW) 27. The section was counterstained with hematoxylin/eosin (HE) *Scale bar* = 8 μm. **h**. Comparison of *S100a6 vs*. *Cacybp* mRNA (*left*) and protein (*right*) levels in cultured neurons *vs*. astrocytes. mRNA expression was normalized to *Gapdh*, a housekeeping gene. *** $p < 0.001$ Student's *t*-test; means ± s.d. from $n = 3$ independent experiments.

Figure 2. Astrocyte-derived S100A6 limits neuritogenesis. a. Cultured mouse astrocytes were stimulated with glutamate (100 μM) *vs*. control. Data were normalized to cell density prior to glutamate exposure on day 1. **b**. Western analysis of S100A6 levels in culture media upon glutamate (100 μM) exposure for 6 h. (1 h, $p = 0.079$; 2 h, *$p = 0.01$; 4 h, *$p = 0.011$; 6 h, **$p = 0.001$ by one-way ANOVA following by Bonferroni's multiple caparisons test). **c.** Cortical neurons were exposed to His-tagged recombinant S100A6 for 30 min and double-labelled for CaCyBp (in magenta) and anti-Histag (in green) antibodies. *Arrows* denote membrane-bound S100A6. DAPI nuclear counterstain was color-coded in blue. *Scale bar* = 8 μm. **d**. CaCyBp was detected in both cytosol and membrane fractions by Western blotting after subcellular fractionation. **e.** Morphometric analysis of cortical neurons exposed to recombinant His-tagged S100A6 (1 μg) for 4 DIV. Data were normalized to neurite length prior to S100A6 exposure on day 1. S100A6 reduced neurite complexity. 'Body cluster area' refers to the surface occupancy of neurons after 4 DIV and is taken as a measure of cell survival. *$p < 0.05$, Student's *t*-test. **f.** CaCyBp in cortical neurons was reduced after recombinant S100A6 (1 μg) exposure for 4 DIV. *$p < 0.05$, Student's *t*-test. **g**. Neuritogenesis of cortical neurons (P0) was reduced 15 days after exposure to shRNA for CaCyBp (shCaCyBp). Primary neurite length (μm) was normalized to mock-transfected controls. ***$p < 0.001$, Student's *t*-test.

Figure 3. CaCyBp regulates protein turnover in neurons. a. CaCyBp accumulates around the endoplasmic reticulum (red asterisks) in hippocampal neurons. *Scale bar* = 500 nm. **b.** Western analysis of total protein content in P0 cortical neurons after sh*Cacybp* exposure. **$p < 0.01$, Student's *t*-test. **c.** mRNA levels for *Gpr78* (*$p = 0.024$), *Atf4*, *Atf6a* (*$p = 0.049$), *Chop*, *Xbp1u* (*$p = 0.048$) and *Xbp1s* (*$p = 0.012$) in P0 cortical neurons after sh*Cacybp* exposure. Data were normalized to *Gapdh*, a housekeeping standard. **d.** Western blot detection of acetylated tubulin (at 50kDa) in cortical neurons exposed to sh*Cacybp* (**$p = 0.006$, Student's *t*-test). **e**. S100A6 in the cytosol of astrocytes (*left*) and cell-free culture medium (*right*) after treatment with EPA (30 μM) for 6 h. Quantitative data are from quadruple experiments; *$p < 0.02$, **$p = 0.0013$, Student's *t*-test. **f.** Classification of significantly altered proteins in mixed sex embryos through primary function assignment by gene ontology. Dams were exposed to a hypercaloric diet enriched in ω-3 PUFAs (**Supplementary Table 1**). **g.** Topmost modified proteins targets, with CaCyBp significantly down-regulated

after gestation experimental diet exposure. In contrast, S100A6 was up-regulated. Only proteins contributing to the morphological differentiation of neurons are shown (*see also* **Supplementary Table 2**). **h.** Western analysis of S100A6 and CaCyBp protein levels (**$p < 0.01$; Student's *t*-test) in the cerebri of male embryos on E18.5 after gestational exposure to an experimental diet *vs*. controls. Data were normalized to total protein load. **i.** Total protein content of cerebral tissues from male embryos at E18.5. *$p < 0.05$; Student's *t*-test. **j.** Western analysis of Acetylated tubulin (at 50 kDa) in the cerebral cortex of male embryos at E18.5 in control and after exposure to an experimental diet. **$p < 0.002$; Student's *t*-test.

Supplementary Figure 1. S100A6 and CaCyBp expression in the cerebral cortex during pre- and postnatal life. a. *S100a6* expression during fetal brain development. mRNAs were quantified by qPCR and normalized to *Gapdh* as a housekeeping standard. (E18.5: *$p < 0.05$, P120: **$p = 0.01$ *vs*. E14.5). **b**. Representative example of S100A6 and CaCyBp protein levels during pre- and postnatal life. Data were normalized to the total protein content of the samples. **c.** Quantitative data for S100A6 (E18.5, P120: **$p < 0.01$ *vs*. E14.5). **d**. *Cacybp* mRNA expression during fetal brain development, normalized against *Gapdh.* *$p < 0.05$ *vs*. E14.5. **e**. CaCyBp protein levels in the mouse cerebral cortex at the ages indicated (P120: **$p < 0.001$) All data were expressed as means ± s.d.; n = 3-4 mice/age. Statistical significance was determined by one-way ANOVA following by Bonferroni multiple caparisons test throughout.

Supplementary Figure 2. Intracellular S100A6 variations and validation of knock-down experiments. a. (*top*) Representative Western blot of S100A6 in the cytosol of astrocytes after glutamate exposure (100 μM) for 6 h. (*bottom*) Quantitative data on intracellular S100A6 levels (2,6 h: *$p < 0.05$). Data were analyzed by one-way ANOVA followed by Bonferroni's multiple caparisons test. Data were expressed as means ± s.d. from n = 3 independent experiments. **b.** (*top*) Total protein content of cytosol and membrane fractions after subcellular fractionation. (*bottom*) Western blot of AMPA receptor subunit 2 (GluA2), synaptosomal-associated protein 25 (SNAP25), translocase of the outer mitochondrial membrane 20 (TOM20), and vesicle-associated membrane protein 2 (VAMP2) in the cytosol *vs*. membrane fractions used to justify subcellular enrichment. **c.** Representative images of cortical neurons 15 days after being transfected with either scrambled shRNA (control) or shRNA against CaCyBp (sh*Cacybp*). Constructs were tagged with green fluorescence protein to validate expression efficacy (*bottom row*). *Scale bars* = 200 μm. **d**. (*top*) *Cacybp* expression in cortical neurons transfected with sh*Cacybp* for 15 days. mRNA levels were quantified by qPCR and normalized to *Gapdh* used as a housekeeping standard. **$p = 0.0097$, Student's *t*-test. Data were expressed as means ± s.d. from n = 3 independent experiments. (*middle*) Western analysis of CaCyBp protein content from the same experiment. *$p = 0.0281$, by one-way ANOVA following by Bonferroni multiple caparisons test. Data were expressed as means ± s.d. from n = 3 independent experiments. (*bottom*) Example of a Western blot for CaCyBp.

Supplementary Figure 3. Recombinant S100A6 affects the UPR machinery. a. Electron microscopy images of negative control, and CaCyBp localization in the vicinity of the endoplasmic reticulum (red asterisks) of neurons in the dentate gyrus of the adult mouse brain. *Scale bars* = 500 nm (12,500x) and 1 μm (6,200x). **b.** Total protein content after exposure to recombinant S100A6 (1 μg) for 24 h *in vitro.* *$p < 0.05$, Student's *t*-test. **c**. Western blot detection of acetylated tubulin (at 50kDa) in cortical neurons after treatment with recombinant S100A6 for 24 h. **$p = 0.028$, Student's *t*-test. **d.** *Gpr78* (*$p = 0.036$), *Atf4*, *Atf6a* (*$p = 0.016$), *Chop*, *Xbp1u* (*$p = 0.036$), *Xbp1s* (*$p = 0.048$) mRNA levels in cortical neurons after exposure to recombinant S100A6 for 24 h. Data were normalized to *Gapdh* used as a housekeeping standard. Data were expressed as means ± s.d.; from n = 3 independent experiments. **e.** Confluence of cortical astrocytes exposed to EPA

at 5 μM-30 μM concentrations for 24 h. Changes in astrocyte density were monitored by live-cell imaging. Data were normalized to cell density prior to EPA exposure on day 1. **f.** Astroglia viability (MTT assay) upon exposure to increasing concentrations of EPA for 24 h; 5 μM: $^{**}p < 0.0001$; 10 μM: $^{*}p = 0.014$; 30 μM: $^{**}p < 0.0001$ (one-way ANOVA followed by Bonferroni's multiple caparisons test). Data were expressed as means ± s.d. from $n = 3$ independent experiments.

Supplementary Table 1. Composition of the hypercaloric and control diets used in this study. Deviation in composition between batches of the diets did not exceed 1% per constituent. Data are from Special Diet Services (UK) and were produced by mass-spectrometry as part of the standard quality control process.

Supplementary Table 2. Proteins with levels significantly modified in the cortices of male mouse fetuses after gestational exposure to a hypercaloric diet. Comparative analysis of $n = 3$ (ω-3 PUFA/vehicle) with data expressed as percentage deviation from the mean control value. Hits with statistically significant differences were only included, as evaluated by the Wilcoxon signed-rank test.

Supplementary Table 3. Antibodies used for immunofluorescence histochemistry and Western blotting. Application-specific dilution, hosts, and vendors of the antibodies deployed in this study were stated.

Supplementary Table 4. Primer sequences used in this study. qPCR reactions were performed with primer pairs amplifying short fragments for each gene. Primer pairs were custom designed to efficiently anneal to homologous nucleotide sequences from mouse.

Cinquina *et al.* - Figure 1

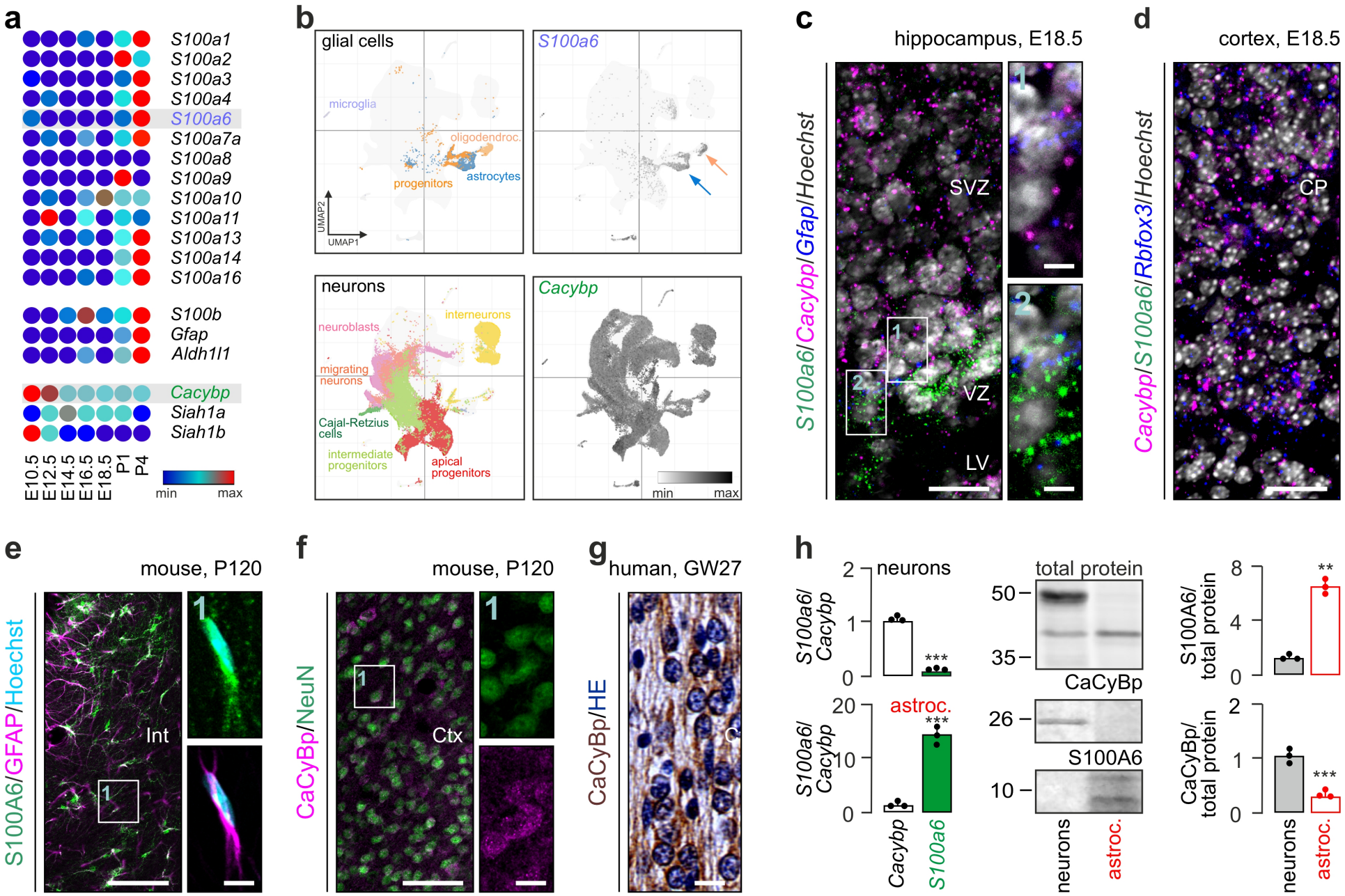

Cinquina *et al*. - Figure 2

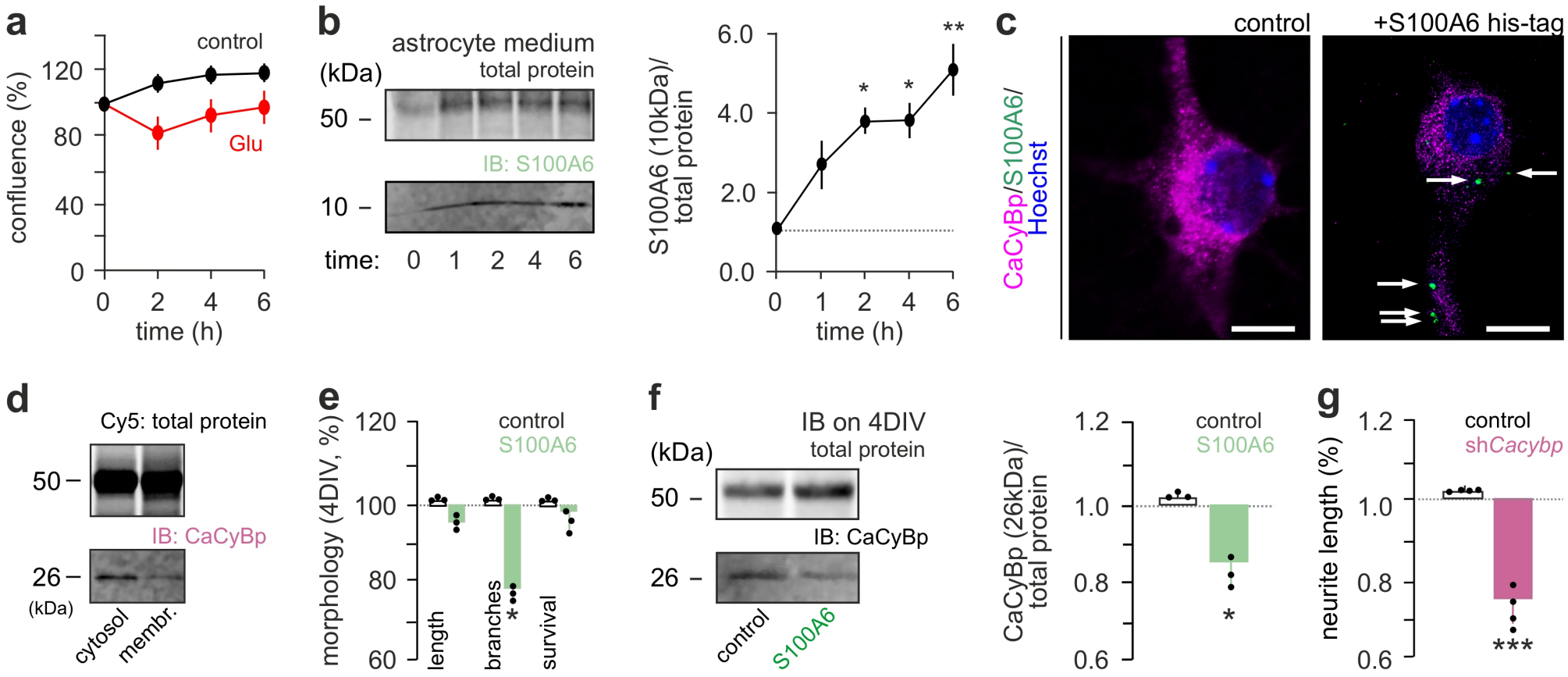

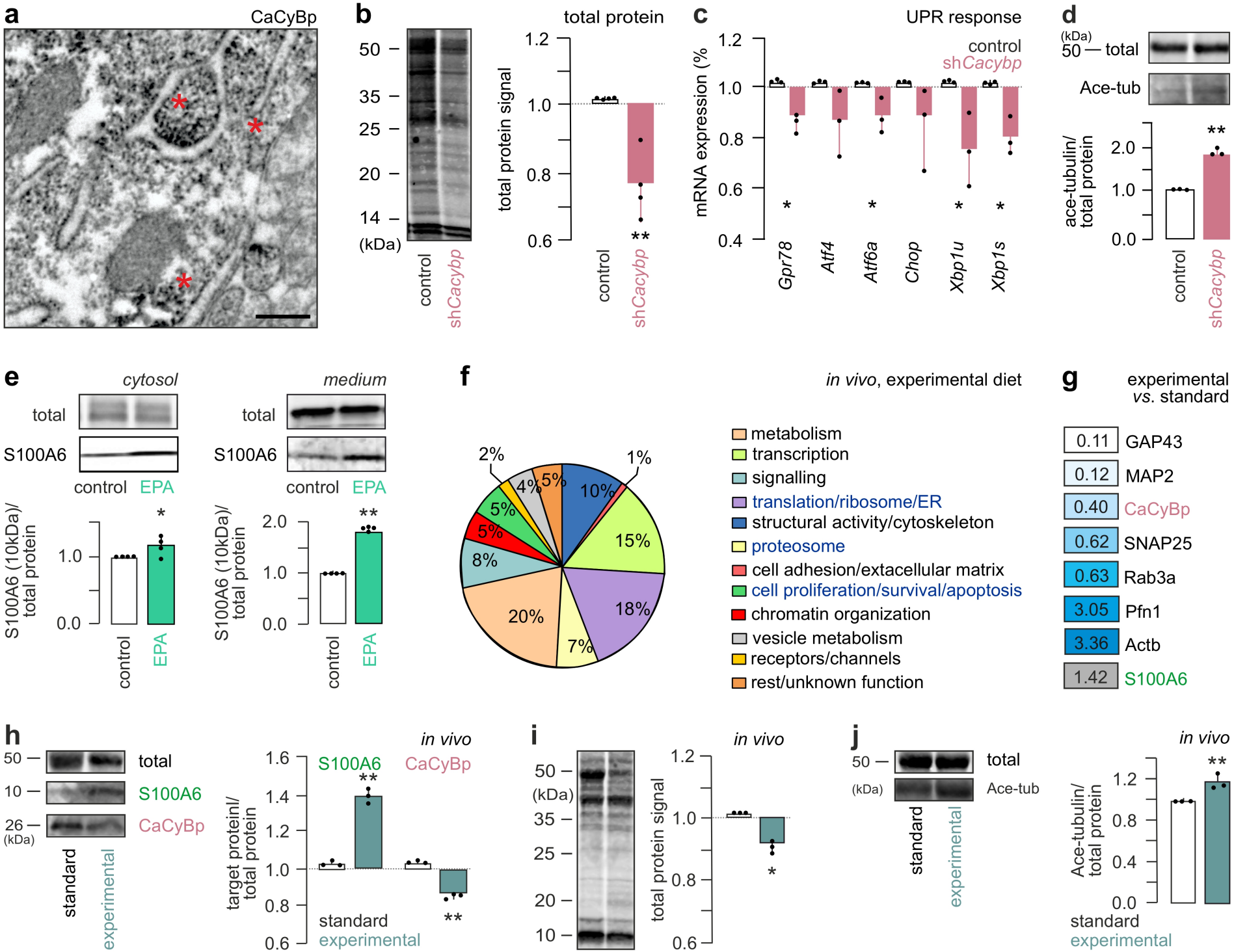
a
CaCyBp
b
total protein
50
35
25
20
14
(kDa)
control
shCacybp
total protein signal
1.2
1.0
0.8
0.6
**
c
UPR response
control
shCacybp
mRNA expression (%
1.2
1.0
0.8
0.6
0.4
Gpr78
Atf4
Atf6a
Chop
Xbp1u
Xbp1s
d
(kDa)
50 — total
Ace-tub
ace-tubulin/
total protein
2.0
1.0
0.0
**
control
shCacybp
e
cytosol
medium
total
S100A6
control
EPA
S100A6 (10kDa)/
total protein
1.0
0.0
2.0
*
**
f
in vivo, experimental diet
2%
1%
4%
5%
10%
5%
5%
15%
8%
20%
18%
7%
metabolism
transcription
signalling
translation/ribosome/ER
structural activity/cytoskeleton
proteosome
cell adhesion/extacellular matrix
cell proliferation/survival/apoptosis
chromatin organization
vesicle metabolism
receptors/channels
rest/unknown function
g
experimental
vs. standard
0.11 GAP43
0.12 MAP2
0.40 CaCyBp
0.62 SNAP25
0.63 Rab3a
3.05 Pfn1
3.36 Actb
1.42 S100A6
h
50 — total
10 — S100A6
26 — CaCyBp
(kDa)
standard
experimental
in vivo
target protein/
total protein
1.6
1.4
1.2
1.0
0.8
0.6
S100A6
CaCyBp
**
i
in vivo
50
(kDa)
35
25
20
10
total protein signal
1.2
1.0
0.8
0.6
*
j
50 — total
(kDa) Ace-tub
standard
experimental
in vivo
Ace-tubulin/
total protein
1.2
0.8
0.4
0.0
**

Cinquina *et al*. - Supplementary Fig. 1

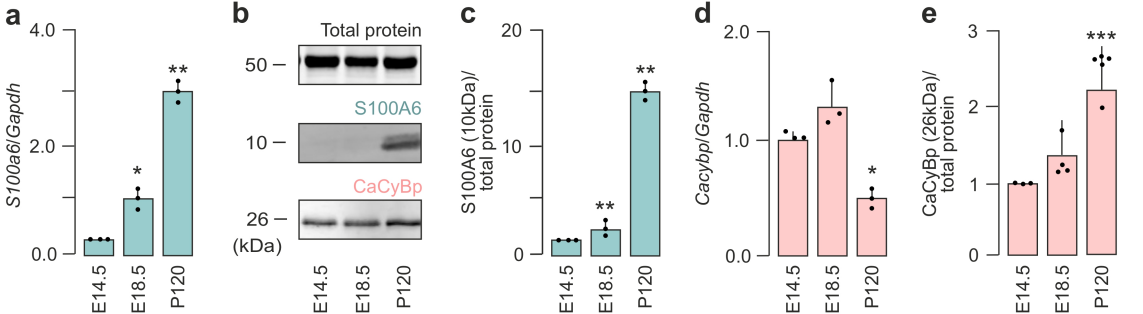

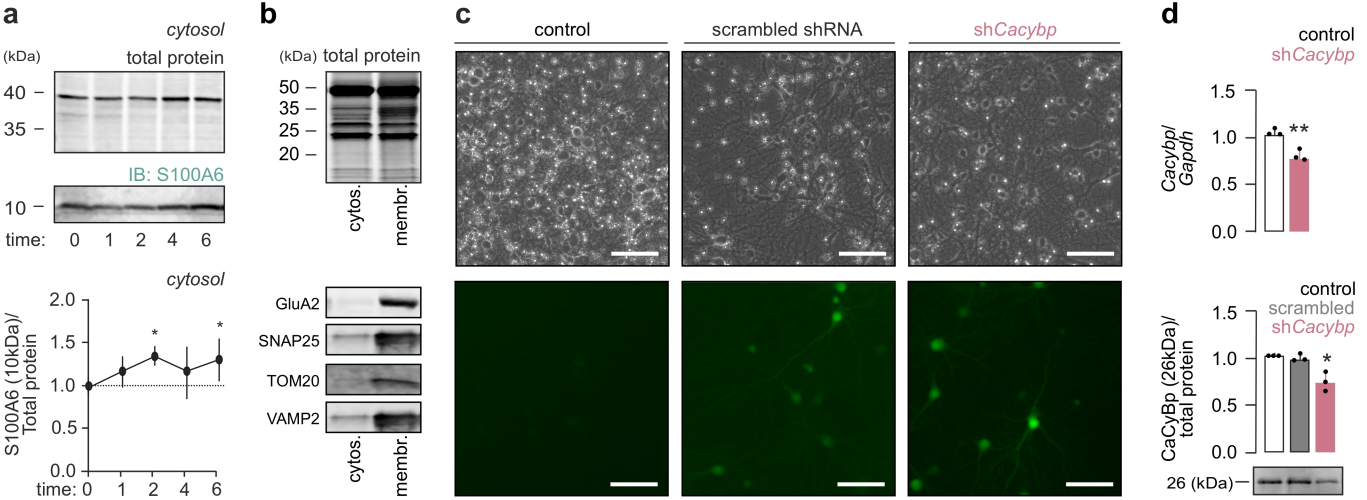
a
cytosol
(kDa)
total protein
40 –
35 –
IB: S100A6
10 –
time: 0 1 2 4 6
cytosol
S100A6 (10kDa)/ Total protein
2.0
1.5
1.0
0.5
0.0
time: 0 1 2 4 6
b
(kDa) total protein
50 –
35 –
25 –
20 –
cytos.
membr.
GluA2
SNAP25
TOM20
VAMP2
cytos.
membr.
c
control
scrambled shRNA
shCacybp
d
control
shCacybp
Cacybp/ Gapdh
1.5
1.0
0.5
0.0
control
scrambled
shCacybp
CaCyBp (26kDa)/ total protein
26 (kDa)

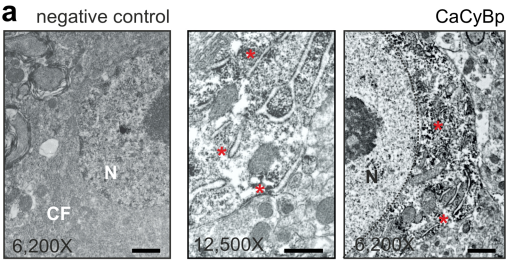
a
negative control
CaCyBp
N
CF
6,200X
12,500X
N
6,200X

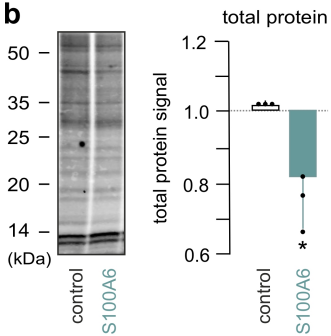
b
total protein
50
35
25
20
14
(kDa)
total protein signal
1.2
1.0
0.8
0.6
control
S100A6
control
S100A6

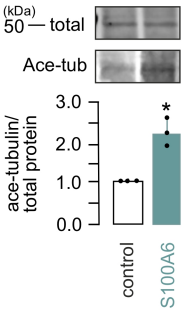
c
(kDa)
50
total
Ace-tub
ace-tubulin/
total protein
3.0
2.0
1.0
0.0
control
S100A6

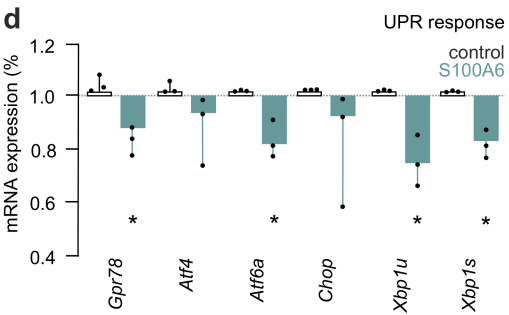
d
UPR response
control
S100A6
mRNA expression (%
1.2
1.0
0.8
0.6
0.4
Gpr78
Atf4
Atf6a
Chop
Xbp1u
Xbp1s

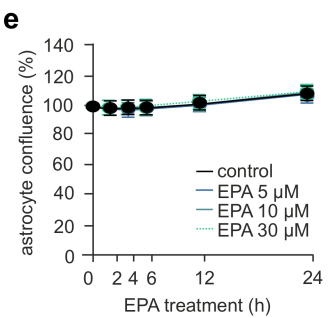
e
astrocyte confluence (%)
140
120
100
80
60
40
20
0
control
EPA 5 µM
EPA 10 µM
EPA 30 µM
0
2 4 6
12
24
EPA treatment (h)

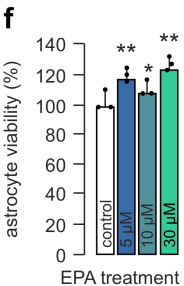
f
astrocyte viability (%)
140
120
100
80
60
40
20
0
control
5 µM
10 µM
30 µM
EPA treatment

Diet batch	Control diet	w-3 diet
Product name	824050	823106
Batch n.		37399
date of manifacture	2005-02-09	2014-08-18
crude fat (CF)	10,00%	34,20%
Kcal/g fresh	3,68%	5,13%
Kcal/g 10% H20	3,47%	4,81%
C18:1 (n6)cis cis-12-Octadecanoic Acid	n.r.	<0,01% CF
C18:1 (n6)trans trans-12-Octadecanoic Acid	n.r.	n.r.
C18:1 (n3)cis	n.r.	<0,01% CF
C18:2 (n6)cis Linoleic acid (LA)	1,34%	10,5% CF
C18:2 (n6)trans Trans Linolelaidic Acid	NA	0,2% CF
C18:3 (n3)cis Aplha-Linolenic Acid (ALA)	**0,23%**	**3,6% CF**
C18:3 (n6)cis Gamma Linoleic Acid	n.r.	0,1% CF
C18:4 (n3)cis Stearidonic Acid	n.r.	1,2% CF
C20:2(n6)cis cis-11,14-Eicosadienoic Acid	n.r.	0,8% CF
C20:3 (n3)cis cis-11,14,17-Eicosatrienoic Acid	n.r.	0,3% CF
C20:3 (n6)cis cis-8,11,14-Eicosatrienoic Acid	n.r.	0,2% CF
C20:4 (n3)cis cis-8,11,14,17-Eicosatetraenoic Acid	n.r.	0,8% CF
C20:4 (n6)cis Arachidonic Acid (AA)	0,01%	0,4% CF
C20:5 (n3)cis Eicosapentenoic Acid (EPA)	**n.r.**	**4,6% CF**
C22:2 (n6)cis Docosadienoic Acid	n.r.	<0,1% CF
C22:3 (n3)cis	n.r.	0,1% CF
C22:4 (n6)cis Docosatetraenoic Acid	n.r.	0,1% CF
C22:5 (n6)cis cis-4,7,10,13,16 Docosapentaenoic Acid	n.r.	0,2% CF
C22:5 (n3)cis Docosapentaenoic acid (DPA)	**n.r.**	**1,7% CF**
C22:6 (n3)cis Docosahexaenoic Acid (DHA)	**n.r.**	**6,0% CF**
C14:1 (n5) cis-9-Myristoleic Acid	0,01%	0,1% CF
C16:1 (n7) cis-9-Palmitoleic Acid	0,07%	3,7% CF
C18:1 (n9) cis Oleic Acid	0,70%	9,13% CF
C12:0 (n3) cis Lauric Acid	0,07%	<0,1% CF
C14:0 (n5) cis-9-Myristic Acid	0,13%	3,3% CF
C16:0 (n7) cis-9-Palmitic Acid	0,23%	11% CF
C18:0 (n6) Stearic Acid	0,14%	2,7% CF
OMEGA 3 FA	**0,26%**	**18,3% CF**
OMEGA 6 FA	**1,87%**	**12,5% CF**
omega3/omega6 ratio	**1:7,2**	**1:0,7**

iTRAQ result: CTR vs W3 proteins (MW test <0.05) list

cell adhesion, extacellular matrix

chipN	Accession	Name	MW test	FOLD in/dec
1	sp|Q9QZQ1|AFAD_MOUSE	Afadin OS=Mus musculus GN=Mllt4 PE=1 SV=3	0,034	**0,705**
2	sp|Q9JII5|DAZP1_MOUSE	DAZ-associated protein 1 OS=Mus musculus GN=Dazap1 PE=2 SV=2	0,034	**0,590**

Cell proliferation/survival/ apoptosis/ cell cycle

47	RRRRRsp|P98083|SHC1_MOUSE	REVERSED SHC-transforming protein 1 OS=Mus musculus GN=Shc1 PE=1 SV=3	0,034	**3,451**
52	sp|P62827|RAN_MOUSE	GTP-binding nuclear protein Ran OS=Mus musculus GN=Ran PE=1 SV=3	0,034	**3,020**
81	sp|Q99MR6|SRRT_MOUSE	Serrate RNA effector molecule homolog OS=Mus musculus GN=Srrt PE=1 SV=1	0,034	**2,000**
95	sp|Q61187|TS101_MOUSE	Tumor susceptibility gene 101 protein OS=Mus musculus GN=Tsg101 PE=1 SV=2	0,034	**1,799**
96	sp|Q61584|FXR1_MOUSE	Fragile X mental retardation syndrome-related protein 1 OS=Mus musculus GN=Fxr1 PI	0,034	**1,758**
2	sp|Q9WVJ2|PSD13_MOUSE	26S proteasome non-ATPase regulatory subunit 13 OS=Mus musculus GN=Psmd13 PE=	0,032	**1,251**
3	sp|P84089|ERH_MOUSE	Enhancer of rudimentary homolog OS=Mus musculus GN=Erh PE=1 SV=1	0,034	**0,682**
13	sp|P97314|CSRP2_MOUSE	Cysteine and glycine-rich protein 2 OS=Mus musculus GN=Csrp2 PE=1 SV=3	0,034	**0,562**
14	sp|Q60865|CAPR1_MOUSE	Caprin-1 OS=Mus musculus GN=Caprin1 PE=1 SV=2	0,034	**0,495**
15	sp|P48678|LMNA_MOUSE	Prelamin-A/C OS=Mus musculus GN=Lmna PE=1 SV=2	0,034	**0,391**
16	sp|Q9CY58|PAIRB_MOUSE	Plasminogen activator inhibitor 1 RNA-binding protein OS=Mus musculus GN=Serbp1	0,034	**0,363**
23	sp|Q9CXI5|MANF_MOUSE	Mesencephalic astrocyte-derived neurotrophic factor OS=Mus musculus GN=Manf PE=	0,032	**0,294**
24	sp|Q9CRB6|TPPP3_MOUSE	Tubulin polymerization-promoting protein family member 3 OS=Mus musculus GN=Tpp	0,034	**0,258**
25	sp|Q922U2|K2C5_MOUSE	Keratin, type II cytoskeletal 5 OS=Mus musculus GN=Krt5 PE=1 SV=1	0,034	**0,089**

DNA/ Chromatin organization

43	sp|P61089|UBE2N_MOUSE	Ubiquitin-conjugating enzyme E2 N OS=Mus musculus GN=Ube2n PE=1 SV=1	0,034	**2,750**
76	sp|Q64511|TOP2B_MOUSE	DNA topoisomerase 2-beta OS=Mus musculus GN=Top2b PE=1 SV=2	0,034	**2,061**
83	sp|Q60973|RBBP7_MOUSE	Histone-binding protein RBBP7 OS=Mus musculus GN=Rbbp7 PE=1 SV=1	0,034	**1,978**
89	sp|Q9CWJ9|PUR9_MOUSE	Bifunctional purine biosynthesis protein PURH OS=Mus musculus GN=Atic PE=1 SV=	0,034	**1,888**
90	sp|Q9DCC4|P5CR3_MOUSE	Pyrroline-5-carboxylate reductase 3 OS=Mus musculus GN=Pycrl PE=2 SV=2	0,032	**1,717**
91	sp|Q9QYI3|DNJC7_MOUSE	DnaJ homolog subfamily C member 7 OS=Mus musculus GN=Dnajc7 PE=1 SV=2	0,034	**1,417**
92	sp|Q8CGY8|OGT1_MOUSE	UDP-N-acetylglucosamine--peptide N-acetylglucosaminyltransferase 110 kDa subunit O	0,032	**1,283**
21	sp|Q9CR41|HYPK_MOUSE	Huntingtin-interacting protein K OS=Mus musculus GN=Hypk PE=2 SV=2	0,032	**0,808**
22	sp|P30681|HMGB2_MOUSE	High mobility group protein B2 OS=Mus musculus GN=Hmgb2 PE=1 SV=3	0,034	**0,399**
23	sp|P43277|H13_MOUSE	Histone H1.3 OS=Mus musculus GN=Hist1h1d PE=1 SV=2	0,034	**0,382**
28	sp|P09405|NUCL_MOUSE	Nucleolin OS=Mus musculus GN=Ncl PE=1 SV=2	0,034	**0,224**
29	sp|P43274|H14_MOUSE	Histone H1.4 OS=Mus musculus GN=Hist1h1e PE=1 SV=2	0,034	**0,184**

Metabolism

44	sp|Q61425|HCDH_MOUSE	Hydroxyacyl-coenzyme A dehydrogenase, mitochondrial OS=Mus musculus GN=Hadh	0,034	**8,235**
49	sp|P16858|G3P_MOUSE	Glyceraldehyde-3-phosphate dehydrogenase OS=Mus musculus GN=Gapdh PE=1 SV=	0,034	**3,321**
54	sp|Q9JII6|AK1A1_MOUSE	Alcohol dehydrogenase [NADP(+)] OS=Mus musculus GN=Akr1a1 PE=1 SV=3	0,032	**2,761**
55	sp|P09411|PGK1_MOUSE	Phosphoglycerate kinase 1 OS=Mus musculus GN=Pgk1 PE=1 SV=4	0,034	**2,742**
57	sp|P29758|OAT_MOUSE	Ornithine aminotransferase, mitochondrial OS=Mus musculus GN=Oat PE=1 SV=1	0,034	**2,737**
58	sp|Q9WUM5|SUCA_MOUSE	Succinyl-CoA ligase [ADP/GDP-forming] subunit alpha, mitochondrial OS=Mus muscul	0,032	**2,510**
60	sp|O08749|DLDH_MOUSE	Dihydrolipoyl dehydrogenase, mitochondrial OS=Mus musculus GN=Dld PE=1 SV=2	0,034	**2,395**

Marker	Dilution	Host	Source
CaCyBp	1:1000	Rabbit	HPA
NeuN	1:500	Mouse	Chemicon
GFAP	1:1000	Guinea Pig	SySy
GluA2	1:200	Guinea Pig	SySy
S100A6 (WB)	1:500	Rabbit	Aviva System Biology
S100A6 (IHC)	1:500	Rabbit	HPA
Anti-V5	1:500	Mouse	Sigma
VAMP2	1:1000	Mouse	SySy
SNAP25	1:1000	Rabbit	SySy
TOM20	1:500	Rabbit	Santa Cruz
Acetilated-Tubulin	1:500	Mouse	Sigma

Gene	Prime sequence	
CaCyBp	(forward)	5’-GGTTGCTCCTCTTACAACAGG-3’
	(reverse)	5’-TGACCTCTCTGTGAAGTGCA-3’
S100a6	(forward)	5’-ACTCTGGCAAGGAAGGTGAC-3’
	(reverse)	5’-GCCGACATACTCCTGGAAGT-3’
Gpr78	(forward)	5’-ACCCTTACTCGGGCCAAATT-3’
	(reverse)	5’-AGAGCGGAACAGGTCCATGT-3’
Atf4	(forward)	5’-ATGGCCGGCTATGGATGAT-3’
	(reverse)	5’-CGAAGTCAAACTCTTTCAGATCCATT -3
Atf6a	(forward)	5’-GGACGAGGTGGTGTCAGAG -3’
	(reverse)	5’-GACAGCTCTTCGCTTTGGAC -3’
Chop	(forward)	5’-CCAACAGAGGTCACACGCAC -3’
	(reverse)	5’-TGACTGGAATCTGGAGAGCGA -3’
Xbp1u	(forward)	5’-GACAGAGAGTCAAACTAACTGGG -3’
	(reverse)	5’-GTCCAGCAGGCAAGAAGGT -3’
Xbp1s	(forward)	5’-GAGTCCGCAGCAGGTG -3’
	(reverse)	5’-GTGTCAGAGTCCATGGGA -3’
Gapdh	(forward)	5’-AACTTTGGCATTGTGGAAGG -3’
	(reverse)	5’-ACACATTGGGGGTAGGAACA -3’

65	sp|O70133|DHX9_MOUSE	ATP-dependent RNA helicase A OS=Mus musculus GN=Dhx9 PE=1 SV=2	0,034	**2,279**
67	sp|Q00612|G6PD1_MOUSE	Glucose-6-phosphate 1-dehydrogenase X OS=Mus musculus GN=G6pdx PE=1 SV=3	0,034	**2,273**
73	sp|P30275|KCRU_MOUSE	Creatine kinase U-type, mitochondrial OS=Mus musculus GN=Ckmt1 PE=1 SV=1	0,034	**2,101**
82	sp|Q9QZ23|NFU1_MOUSE	NFU1 iron-sulfur cluster scaffold homolog, mitochondrial OS=Mus musculus GN=Nfu1	0,032	**1,980**
86	sp|P45376|ALDR_MOUSE	Aldose reductase OS=Mus musculus GN=Akr1b1 PE=1 SV=3	0,031	**1,968**
37	sp|Q9R0P3|ESTD_MOUSE	S-formylglutathione hydrolase OS=Mus musculus GN=Esd PE=2 SV=1	0,032	**1,917**
18	sp|Q3THK7|GUAA_MOUSE	GMP synthase [glutamine-hydrolyzing] OS=Mus musculus GN=Gmps PE=1 SV=2	0,032	**1,846**
24	sp|Q8K2T1|NMRL1_MOUSE	NmrA-like family domain-containing protein 1 OS=Mus musculus GN=Nmral1 PE=1 S	0,034	**1,830**
25	sp|Q9D051|ODPB_MOUSE	Pyruvate dehydrogenase E1 component subunit beta, mitochondrial OS=Mus musculus (	0,034	**1,585**
26	sp|P50247|SAHH_MOUSE	Adenosylhomocysteinase OS=Mus musculus GN=Ahcy PE=1 SV=3	0,034	**1,578**
27	sp|Q8K2B3|DHSA_MOUSE	Succinate dehydrogenase [ubiquinone] flavoprotein subunit, mitochondrial OS=Mus mus	0,034	**1,529**
28	sp|Q9CPV4|GLOD4_MOUSE	Glyoxalase domain-containing protein 4 OS=Mus musculus GN=Glod4 PE=2 SV=1	0,034	**1,528**
29	sp|Q99LC5|ETFA_MOUSE	Electron transfer flavoprotein subunit alpha, mitochondrial OS=Mus musculus GN=Etfa	0,034	**1,452**
30	sp|Q9CQ75|NDUA2_MOUSE	NADH dehydrogenase [ubiquinone] 1 alpha subcomplex subunit 2 OS=Mus musculus G	0,034	**1,396**
31	sp|Q9JI46|NUDT3_MOUSE	Diphosphoinositol polyphosphate phosphohydrolase 1 OS=Mus musculus GN=Nudt3 P	0,034	**1,320**
32	sp|Q8BH95|ECHM_MOUSE	Enoyl-CoA hydratase, mitochondrial OS=Mus musculus GN=Echs1 PE=1 SV=1	0,034	**1,169**
33	sp|Q9Z2I9|SUCB1_MOUSE	Succinyl-CoA ligase [ADP-forming] subunit beta, mitochondrial OS=Mus musculus GN	0,034	**0,876**
34	sp|P23506|PIMT_MOUSE	Protein-L-isoaspartate(D-aspartate) O-methyltransferase OS=Mus musculus GN=Pcmt1	0,032	**0,800**
17	sp|O08795|GLU2B_MOUSE	Glucosidase 2 subunit beta OS=Mus musculus GN=Prkcsh PE=1 SV=1	0,034	**0,697**
18	sp|Q64105|SPRE_MOUSE	Sepiapterin reductase OS=Mus musculus GN=Spr PE=1 SV=1	0,034	**0,687**
19	sp|P62137|PP1A_MOUSE	Serine/threonine-protein phosphatase PP1-alpha catalytic subunit OS=Mus musculus GN	0,034	**0,671**
20	sp|Q9D1K2|VATF_MOUSE	V-type proton ATPase subunit F OS=Mus musculus GN=Atp6v1f PE=1 SV=2	0,034	**0,583**
21	sp|P99028|QCR6_MOUSE	Cytochrome b-c1 complex subunit 6, mitochondrial OS=Mus musculus GN=Uqcrh PE=	0,034	**0,556**
31	sp|O54724|PTRF_MOUSE	Polymerase I and transcript release factor OS=Mus musculus GN=Ptrf PE=1 SV=1	0,034	**0,535**
32	sp|Q9CR21|ACPM_MOUSE	Acyl carrier protein, mitochondrial OS=Mus musculus GN=Ndufab1 PE=1 SV=1	0,032	**0,517**
33	sp|Q9JHU9|INO1_MOUSE	Inositol-3-phosphate synthase 1 OS=Mus musculus GN=Isyna1 PE=2 SV=1	0,034	**0,516**
25	sp|P32020|NLTP_MOUSE	Non-specific lipid-transfer protein OS=Mus musculus GN=Scp2 PE=1 SV=3	0,034	**0,514**
26	sp|Q9CXZ1|NDUS4_MOUSE	NADH dehydrogenase [ubiquinone] iron-sulfur protein 4, mitochondrial OS=Mus muscu	0,034	**0,496**
27	sp|P05202|AATM_MOUSE	Aspartate aminotransferase, mitochondrial OS=Mus musculus GN=Got2 PE=1 SV=1	0,034	**0,476**
36	sp|P07724|ALBU_MOUSE	Serum albumin OS=Mus musculus GN=Alb PE=1 SV=3	0,034	**0,457**
37	sp|Q9D855|QCR7_MOUSE	Cytochrome b-c1 complex subunit 7 OS=Mus musculus GN=Uqcrb PE=1 SV=3	0,034	**0,439**
38	sp|P52503|NDUS6_MOUSE	NADH dehydrogenase [ubiquinone] iron-sulfur protein 6, mitochondrial OS=Mus muscu	0,034	**0,438**
39	sp|Q9DCX2|ATP5H_MOUSE	ATP synthase subunit d, mitochondrial OS=Mus musculus GN=Atp5h PE=1 SV=3	0,034	**0,434**
40	sp|P56480|ATPB_MOUSE	ATP synthase subunit beta, mitochondrial OS=Mus musculus GN=Atp5b PE=1 SV=2	0,034	**0,420**
41	sp|P19536|COX5B_MOUSE	Cytochrome c oxidase subunit 5B, mitochondrial OS=Mus musculus GN=Cox5b PE=1 S	0,034	**0,387**
42	sp|P56391|CX6B1_MOUSE	Cytochrome c oxidase subunit 6B1 OS=Mus musculus GN=Cox6b1 PE=1 SV=2	0,034	**0,372**
14	sp|P62897|CYC_MOUSE	Cytochrome c, somatic OS=Mus musculus GN=Cycs PE=1 SV=2	0,034	**0,358**
15	sp|Q9D6J6|NDUV2_MOUSE	NADH dehydrogenase [ubiquinone] flavoprotein 2, mitochondrial OS=Mus musculus G	0,034	**0,350**
16	sp|Q61545|EWS_MOUSE	RNA-binding protein EWS OS=Mus musculus GN=Ewsr1 PE=1 SV=2	0,034	**0,349**
40	sp|P08228|SODC_MOUSE	Superoxide dismutase [Cu-Zn] OS=Mus musculus GN=Sod1 PE=1 SV=2	0,034	**0,329**
41	sp|Q9DCJ9|NPL_MOUSE	N-acetylneuraminate lyase OS=Mus musculus GN=Npl PE=1 SV=1	0,034	**0,328**
10	sp|Q9D3D9|ATPD_MOUSE	ATP synthase subunit delta, mitochondrial OS=Mus musculus GN=Atp5d PE=1 SV=1	0,034	**0,321**
11	sp|Q61207|SAP_MOUSE	Sulfated glycoprotein 1 OS=Mus musculus GN=Psap PE=1 SV=2	0,034	**0,298**
12	sp|P12787|COX5A_MOUSE	Cytochrome c oxidase subunit 5A, mitochondrial OS=Mus musculus GN=Cox5a PE=1 S	0,034	**0,238**
13	sp|Q64433|CH10_MOUSE	10 kDa heat shock protein, mitochondrial OS=Mus musculus GN=Hspe1 PE=1 SV=2	0,034	**0,235**
14	sp|O35143|ATIF1_MOUSE	ATPase inhibitor, mitochondrial OS=Mus musculus GN=Atpif1 PE=2 SV=2	0,034	**0,228**
11	sp|P97450|ATP5J_MOUSE	ATP synthase-coupling factor 6, mitochondrial OS=Mus musculus GN=Atp5j PE=1 SV=	0,034	**0,204**

Proteosome / protein degradation/exosome

45	sp|P62196|PRS8_MOUSE	26S protease regulatory subunit 8 OS=Mus musculus GN=Psmc5 PE=1 SV=1	0,034	**3,984**
1	sp|Q8BG32|PSD11_MOUSE	26S proteasome non-ATPase regulatory subunit 11 OS=Mus musculus GN=Psmd11 PE	0,034	**2,561**
3	sp|Q99JI4|PSMD6_MOUSE	26S proteasome non-ATPase regulatory subunit 6 OS=Mus musculus GN=Psmd6 PE=1	0,034	**2,073**
4	sp|Q7TQI3|OTUB1_MOUSE	Ubiquitin thioesterase OTUB1 OS=Mus musculus GN=Otub1 PE=1 SV=2	0,034	**1,731**
5	sp|Q8CGK3|LONM_MOUSE	Lon protease homolog, mitochondrial OS=Mus musculus GN=Lonp1 PE=1 SV=2	0,034	**1,606**
6	sp|Q3TXS7|PSMD1_MOUSE	26S proteasome non-ATPase regulatory subunit 1 OS=Mus musculus GN=Psmd1 PE=1	0,034	**1,597**
7	sp|Q11011|PSA_MOUSE	Puromycin-sensitive aminopeptidase OS=Mus musculus GN=Npepps PE=1 SV=2	0,034	**1,435**
8	sp|Q922Y1|UBXN1_MOUSE	UBX domain-containing protein 1 OS=Mus musculus GN=Ubxn1 PE=1 SV=1	0,034	**1,361**
9	sp|P68037|UB2L3_MOUSE	Ubiquitin-conjugating enzyme E2 L3 OS=Mus musculus GN=Ube2l3 PE=2 SV=1	0,034	**1,339**
10	sp|P57716|NICA_MOUSE	Nicastrin OS=Mus musculus GN=Ncstn PE=1 SV=3	0,034	**0,793**
11	sp|Q91VX2|UBAP2_MOUSE	Ubiquitin-associated protein 2 OS=Mus musculus GN=Ubap2 PE=2 SV=1	0,034	**0,722**
9	sp|Q9Z2W0|DNPEP_MOUSE	Aspartyl aminopeptidase OS=Mus musculus GN=Dnpep PE=2 SV=2	0,034	**0,708**
7	sp|Q00898|A1AT5_MOUSE	Alpha-1-antitrypsin 1-5 OS=Mus musculus GN=Serpina1e PE=1 SV=1	0,034	**0,607**
8	sp|Q9CQK7|RWDD1_MOUSE	RWD domain-containing protein 1 OS=Mus musculus GN=Rwdd1 PE=1 SV=1	0,034	**0,596**
9	sp|P62334|PRS10_MOUSE	26S protease regulatory subunit 10B OS=Mus musculus GN=Psmc6 PE=1 SV=1	0,034	**0,482**
10	sp|P97371|PSME1_MOUSE	Proteasome activator complex subunit 1 OS=Mus musculus GN=Psme1 PE=2 SV=2	0,034	**0,464**
11	sp|Q9CXW3|CYBP_MOUSE	Calcyclin-binding protein OS=Mus musculus GN=Cacybp PE=1 SV=1	0,034	**0,430**
12	sp|Q80X50|UBP2L_MOUSE	Ubiquitin-associated protein 2-like OS=Mus musculus GN=Ubap2l PE=1 SV=1	0,034	**0,413**

RNA metabolism / transcription

59	sp|Q99K48|NONO_MOUSE	Non-POU domain-containing octamer-binding protein OS=Mus musculus GN=Nono PE	0,034	**2,423**
63	sp|Q6PB66|LPPRC_MOUSE	Leucine-rich PPR motif-containing protein, mitochondrial OS=Mus musculus GN=Lrppr	0,034	**2,326**
66	sp|O08784|TCOF_MOUSE	Treacle protein OS=Mus musculus GN=Tcof1 PE=1 SV=1	0,034	**2,275**
68	sp|Q8R409|HEXI1_MOUSE	Protein HEXIM1 OS=Mus musculus GN=Hexim1 PE=1 SV=1	0,034	**2,259**
71	sp|Q99LF4|RTCB_MOUSE	tRNA-splicing ligase RtcB homolog OS=Mus musculus GN=D10Wsu52e PE=2 SV=1	0,034	**2,174**
72	sp|Q9CQL1|MGN2_MOUSE	Protein mago nashi homolog 2 OS=Mus musculus GN=Magohb PE=2 SV=1	0,032	**2,138**
79	sp|P59999|ARPC4_MOUSE	Actin-related protein 2/3 complex subunit 4 OS=Mus musculus GN=Arpc4 PE=1 SV=3	0,032	**2,050**
87	sp|Q9D4J7|PHF6_MOUSE	PHD finger protein 6 OS=Mus musculus GN=Phf6 PE=1 SV=1	0,034	**1,963**
92	sp|Q62376|RU17_MOUSE	U1 small nuclear ribonucleoprotein 70 kDa OS=Mus musculus GN=Snrnp70 PE=1 SV=	0,034	**1,862**
93	sp|P28352|APEX1_MOUSE	DNA-(apurinic or apyrimidinic site) lyase OS=Mus musculus GN=Apex1 PE=1 SV=2	0,034	**1,755**
94	sp|Q9D554|SF3A3_MOUSE	Splicing factor 3A subunit 3 OS=Mus musculus GN=Sf3a3 PE=2 SV=2	0,034	**1,723**
95	sp|Q3UJB9|EDC4_MOUSE	Enhancer of mRNA-decapping protein 4 OS=Mus musculus GN=Edc4 PE=1 SV=2	0,032	**1,715**
96	sp|Q501J6|DDX17_MOUSE	Probable ATP-dependent RNA helicase DDX17 OS=Mus musculus GN=Ddx17 PE=2 S	0,034	**1,624**
97	sp|Q9WTM5|RUVB2_MOUSE	RuvB-like 2 OS=Mus musculus GN=Ruvbl2 PE=2 SV=3	0,034	**1,528**
98	sp|Q569Z6|TR150_MOUSE	Thyroid hormone receptor-associated protein 3 OS=Mus musculus GN=Thrap3 PE=1 S	0,034	**1,519**
99	sp|P11499|HS90B_MOUSE	Heat shock protein HSP 90-beta OS=Mus musculus GN=Hsp90ab1 PE=1 SV=3	0,034	**1,501**
34	sp|Q99M28|RNPS1_MOUSE	RNA-binding protein with serine-rich domain 1 OS=Mus musculus GN=Rnps1 PE=2 S	0,034	**1,472**
35	sp|Q9JKR6|HYOU1_MOUSE	Hypoxia up-regulated protein 1 OS=Mus musculus GN=Hyou1 PE=1 SV=1	0,034	**1,468**
36	sp|Q9D0T1|NH2L1_MOUSE	NHP2-like protein 1 OS=Mus musculus GN=Nhp2l1 PE=2 SV=4	0,034	**1,411**
37	sp|Q9Z1Z2|STRAP_MOUSE	Serine-threonine kinase receptor-associated protein OS=Mus musculus GN=Strap PE=1	0,034	**1,381**
38	sp|Q9WUK6|ZN238_MOUSE	Zinc finger protein 238 OS=Mus musculus GN=Znf238 PE=2 SV=1	0,032	**1,372**
39	sp|Q01147|CREB1_MOUSE	Cyclic AMP-responsive element-binding protein 1 OS=Mus musculus GN=Creb1 PE=1	0,034	**1,371**
33	sp|Q8C2Q3|RBM14_MOUSE	RNA-binding protein 14 OS=Mus musculus GN=Rbm14 PE=1 SV=1	0,034	**1,310**
34	sp|Q8K4Z5|SF3A1_MOUSE	Splicing factor 3A subunit 1 OS=Mus musculus GN=Sf3a1 PE=1 SV=1	0,034	**1,274**
35	sp|O08756|HCD2_MOUSE	3-hydroxyacyl-CoA dehydrogenase type-2 OS=Mus musculus GN=Hsd17b10 PE=1 SV	0,034	**1,273**
12	sp|P53996|CNBP_MOUSE	Cellular nucleic acid-binding protein OS=Mus musculus GN=Cnbp PE=2 SV=2	0,034	**0,729**
38	sp|Q9CSN1|SNW1_MOUSE	SNW domain-containing protein 1 OS=Mus musculus GN=Snw1 PE=1 SV=3	0,034	**0,690**

39	sp|O35381|AN32A_MOUSE	Acidic leucine-rich nuclear phosphoprotein 32 family member A OS=Mus musculus GN	0,034	**0,688**
40	sp|Q9D1J3|SARNP_MOUSE	SAP domain-containing ribonucleoprotein OS=Mus musculus GN=Sarnp PE=1 SV=3	0,032	**0,679**
15	sp|Q61701|ELAV4_MOUSE	ELAV-like protein 4 OS=Mus musculus GN=Elavl4 PE=1 SV=1	0,034	**0,639**
16	sp|Q8BJH1|ZC21A_MOUSE	Zinc finger C2HC domain-containing protein 1A OS=Mus musculus GN=Zc2hc1a PE=2	0,034	**0,599**
17	sp|P51859|HDGF_MOUSE	Hepatoma-derived growth factor OS=Mus musculus GN=Hdgf PE=1 SV=2	0,034	**0,586**
18	sp|Q9CQQ8|LSM7_MOUSE	U6 snRNA-associated Sm-like protein LSm7 OS=Mus musculus GN=Lsm7 PE=2 SV=1	0,034	**0,506**
35	sp|O35326|SRSF5_MOUSE	Serine/arginine-rich splicing factor 5 OS=Mus musculus GN=Srsf5 PE=1 SV=2	0,034	**0,485**
36	sp|Q3UL36|ARGL1_MOUSE	Arginine and glutamate-rich protein 1 OS=Mus musculus GN=Arglu1 PE=1 SV=2	0,034	**0,443**
37	sp|Q80ZM7|T2AG_MOUSE	Transcription initiation factor IIA subunit 2 OS=Mus musculus GN=Gtf2a2 PE=2 SV=2	0,034	**0,402**
38	sp|P62500|T22D1_MOUSE	TSC22 domain family protein 1 OS=Mus musculus GN=Tsc22d1 PE=2 SV=2	0,034	**0,357**
39	sp|O08583|THOC4_MOUSE	THO complex subunit 4 OS=Mus musculus GN=Alyref PE=1 SV=3	0,034	**0,354**
40	sp|Q62093|SRSF2_MOUSE	Serine/arginine-rich splicing factor 2 OS=Mus musculus GN=Srsf2 PE=1 SV=4	0,034	**0,352**
20	sp|P17095|HMGA1_MOUSE	High mobility group protein HMG-I/HMG-Y OS=Mus musculus GN=Hmga1 PE=1 SV=	0,034	**0,267**
26	sp|P62960|YBOX1_MOUSE	Nuclease-sensitive element-binding protein 1 OS=Mus musculus GN=Ybx1 PE=1 SV=3	0,034	**0,266**

Signalling

62	sp|P61027|RAB10_MOUSE	Ras-related protein Rab-10 OS=Mus musculus GN=Rab10 PE=1 SV=1	0,034	**2,364**
77	sp|Q61598|GDIB_MOUSE	Rab GDP dissociation inhibitor beta OS=Mus musculus GN=Gdi2 PE=1 SV=1	0,034	**2,053**
84	sp|P11103|PARP1_MOUSE	Poly [ADP-ribose] polymerase 1 OS=Mus musculus GN=Parp1 PE=1 SV=3	0,034	**1,972**
90	sp|Q8CIN4|PAK2_MOUSE	Serine/threonine-protein kinase PAK 2 OS=Mus musculus GN=Pak2 PE=1 SV=1	0,034	**1,884**
91	sp|P58389|PTPA_MOUSE	Serine/threonine-protein phosphatase 2A activator OS=Mus musculus GN=Ppp2r4 PE=1	0,034	**1,766**
92	sp|Q8BK63|KC1A_MOUSE	Casein kinase I isoform alpha OS=Mus musculus GN=Csnk1a1 PE=2 SV=2	0,034	**1,554**
93	sp|P84084|ARF5_MOUSE	ADP-ribosylation factor 5 OS=Mus musculus GN=Arf5 PE=2 SV=2	0,034	**1,546**
94	sp|Q9JIF0|ANM1_MOUSE	Protein arginine N-methyltransferase 1 OS=Mus musculus GN=Prmt1 PE=1 SV=1	0,034	**1,544**
95	sp|Q3UM45|PP1R7_MOUSE	Protein phosphatase 1 regulatory subunit 7 OS=Mus musculus GN=Ppp1r7 PE=1 SV=2	0,034	**1,478**
96	sp|P46935|NEDD4_MOUSE	E3 ubiquitin-protein ligase NEDD4 OS=Mus musculus GN=Nedd4 PE=1 SV=3	0,034	**1,304**
97	sp|P05132|KAPCA_MOUSE	cAMP-dependent protein kinase catalytic subunit alpha OS=Mus musculus GN=Prkaca	0,034	**1,297**
98	sp|Q9CQZ1|HSBP1_MOUSE	Heat shock factor-binding protein 1 OS=Mus musculus GN=Hsbp1 PE=2 SV=1	0,034	**0,690**
99	sp|Q9DBG9|TX1B3_MOUSE	Tax1-binding protein 3 OS=Mus musculus GN=Tax1bp3 PE=1 SV=1	0,034	**0,673**
100	sp|Q99MI1|RB6I2_MOUSE	ELKS/Rab6-interacting/CAST family member 1 OS=Mus musculus GN=Erc1 PE=1 SV	0,034	**0,669**
29	sp|P26883|FKB1A_MOUSE	Peptidyl-prolyl cis-trans isomerase FKBP1A OS=Mus musculus GN=Fkbp1a PE=1 SV=	0,034	**0,664**
30	sp|Q60864|STIP1_MOUSE	Stress-induced-phosphoprotein 1 OS=Mus musculus GN=Stip1 PE=1 SV=1	0,034	**0,610**
31	sp|Q9WTQ5|AKA12_MOUSE	A-kinase anchor protein 12 OS=Mus musculus GN=Akap12 PE=1 SV=1	0,034	**0,596**
32	sp|Q91WK0|LRRF2_MOUSE	Leucine-rich repeat flightless-interacting protein 2 OS=Mus musculus GN=Lrrfip2 PE=1	0,034	**0,537**
33	sp|Q62048|PEA15_MOUSE	Astrocytic phosphoprotein PEA-15 OS=Mus musculus GN=Pea15 PE=1 SV=1	0,034	**0,479**
34	sp|Q61937|NPM_MOUSE	Nucleophosmin OS=Mus musculus GN=Npm1 PE=1 SV=1	0,034	**0,445**
35	sp|P62761|VISL1_MOUSE	Visinin-like protein 1 OS=Mus musculus GN=Vsnl1 PE=1 SV=2	0,034	**0,254**

Structural molecule /cytoskeleton/axon growth and guidance

46	sp|P13541|MYH3_MOUSE	Myosin-3 OS=Mus musculus GN=Myh3 PE=2 SV=2	0,034	**3,855**
48	sp|P60710|ACTB_MOUSE	Actin, cytoplasmic 1 OS=Mus musculus GN=Actb PE=1 SV=1	0,034	**3,360**
51	sp|P62962|PROF1_MOUSE	Profilin-1 OS=Mus musculus GN=Pfn1 PE=1 SV=2	0,034	**3,053**
61	sp|Q9CVB6|ARPC2_MOUSE	Actin-related protein 2/3 complex subunit 2 OS=Mus musculus GN=Arpc2 PE=1 SV=3	0,034	**2,386**
69	sp|P63168|DYL1_MOUSE	Dynein light chain 1, cytoplasmic OS=Mus musculus GN=Dynll1 PE=1 SV=1	0,034	**2,208**
80	sp|P13542|MYH8_MOUSE	Myosin-8 OS=Mus musculus GN=Myh8 PE=1 SV=2	0,034	**2,017**
94	sp|P26040|EZRI_MOUSE	Ezrin OS=Mus musculus GN=Ezr PE=1 SV=3	0,034	**1,817**
95	sp|O35684|NEUS_MOUSE	Neuroserpin OS=Mus musculus GN=Serpini1 PE=1 SV=1	0,034	**1,681**

96	sp|Q9R0Q6|ARC1A_MOUSE	Actin-related protein 2/3 complex subunit 1A OS=Mus musculus GN=Arpc1a PE=1 SV	0,034	**1,416**
97	sp|Q9Z0H8|CLIP2_MOUSE	CAP-Gly domain-containing linker protein 2 OS=Mus musculus GN=Clip2 PE=1 SV=2	0,034	**1,342**
98	sp|P40124|CAP1_MOUSE	Adenylyl cyclase-associated protein 1 OS=Mus musculus GN=Cap1 PE=1 SV=4	0,034	**1,277**
99	sp|P61164|ACTZ_MOUSE	Alpha-centractin OS=Mus musculus GN=Actr1a PE=2 SV=1	0,034	**1,207**
100	sp|O88342|WDR1_MOUSE	WD repeat-containing protein 1 OS=Mus musculus GN=Wdr1 PE=1 SV=3	0,034	**0,624**
101	sp|Q9DAW9|CNN3_MOUSE	Calponin-3 OS=Mus musculus GN=Cnn3 PE=2 SV=1	0,034	**0,618**
102	sp|Q60598|SRC8_MOUSE	Src substrate cortactin OS=Mus musculus GN=Cttn PE=1 SV=2	0,034	**0,607**
30	sp|Q8BQ30|PPR18_MOUSE	Phostensin OS=Mus musculus GN=Ppp1r18 PE=1 SV=1	0,034	**0,555**
31	sp|Q9Z2H5|E41L1_MOUSE	Band 4.1-like protein 1 OS=Mus musculus GN=Epb41l1 PE=1 SV=2	0,034	**0,550**
32	sp|P56395|CYB5_MOUSE	Cytochrome b5 OS=Mus musculus GN=Cyb5a PE=1 SV=2	0,034	**0,548**
33	sp|Q99P72|RTN4_MOUSE	Reticulon-4 OS=Mus musculus GN=Rtn4 PE=1 SV=2	0,034	**0,538**
34	sp|Q60605|MYL6_MOUSE	Myosin light polypeptide 6 OS=Mus musculus GN=Myl6 PE=1 SV=3	0,034	**0,465**
35	sp|Q99KJ8|DCTN2_MOUSE	Dynactin subunit 2 OS=Mus musculus GN=Dctn2 PE=1 SV=3	0,034	**0,461**
36	sp|Q61792|LASP1_MOUSE	LIM and SH3 domain protein 1 OS=Mus musculus GN=Lasp1 PE=1 SV=1	0,034	**0,441**
37	sp|Q9QYC0|ADDA_MOUSE	Alpha-adducin OS=Mus musculus GN=Add1 PE=1 SV=2	0,034	**0,358**
38	sp|Q3UNH4|GRIN1_MOUSE	G protein-regulated inducer of neurite outgrowth 1 OS=Mus musculus GN=Gprin1 PE=	0,034	**0,303**
39	sp|P20357|MAP2_MOUSE	Microtubule-associated protein 2 OS=Mus musculus GN=Map2 PE=1 SV=2	0,034	**0,259**
40	sp|P21107|TPM3_MOUSE	Tropomyosin alpha-3 chain OS=Mus musculus GN=Tpm3 PE=1 SV=2	0,032	**0,230**
41	sp|P14873|MAP1B_MOUSE	Microtubule-associated protein 1B OS=Mus musculus GN=Map1b PE=1 SV=2	0,034	**0,159**

Translation / ribosome assembly / protein biogenesis /ER

53	sp|P53026|RL10A_MOUSE	60S ribosomal protein L10a OS=Mus musculus GN=Rpl10a PE=1 SV=3	0,034	**2,988**
56	sp|Q9D8E6|RL4_MOUSE	60S ribosomal protein L4 OS=Mus musculus GN=Rpl4 PE=1 SV=3	0,032	**2,739**
64	sp|P25444|RS2_MOUSE	40S ribosomal protein S2 OS=Mus musculus GN=Rps2 PE=1 SV=3	0,034	**2,305**
70	sp|P62918|RL8_MOUSE	60S ribosomal protein L8 OS=Mus musculus GN=Rpl8 PE=2 SV=2	0,032	**2,198**
74	sp|Q8BHN3|GANAB_MOUSE	Neutral alpha-glucosidase AB OS=Mus musculus GN=Ganab PE=1 SV=1	0,034	**2,086**
75	sp|Q9CR16|PPID_MOUSE	Peptidyl-prolyl cis-trans isomerase D OS=Mus musculus GN=Ppid PE=1 SV=3	0,034	**2,069**
78	sp|P12970|RL7A_MOUSE	60S ribosomal protein L7a OS=Mus musculus GN=Rpl7a PE=2 SV=2	0,034	**2,053**
85	sp|Q61699|HS105_MOUSE	Heat shock protein 105 kDa OS=Mus musculus GN=Hsph1 PE=1 SV=2	0,034	**1,972**
88	sp|Q8BK64|AHSA1_MOUSE	Activator of 90 kDa heat shock protein ATPase homolog 1 OS=Mus musculus GN=Ahs	0,034	**1,903**
91	sp|P47911|RL6_MOUSE	60S ribosomal protein L6 OS=Mus musculus GN=Rpl6 PE=1 SV=3	0,034	**1,884**
96	sp|P62830|RL23_MOUSE	60S ribosomal protein L23 OS=Mus musculus GN=Rpl23 PE=1 SV=1	0,034	**1,792**
97	sp|Q61576|FKB10_MOUSE	Peptidyl-prolyl cis-trans isomerase FKBP10 OS=Mus musculus GN=Fkbp10 PE=1 SV=	0,034	**1,782**
98	sp|P35564|CALX_MOUSE	Calnexin OS=Mus musculus GN=Canx PE=1 SV=1	0,034	**1,778**
99	sp|P62281|RS11_MOUSE	40S ribosomal protein S11 OS=Mus musculus GN=Rps11 PE=2 SV=3	0,034	**1,771**
100	sp|P14869|RLA0_MOUSE	60S acidic ribosomal protein P0 OS=Mus musculus GN=Rplp0 PE=1 SV=3	0,034	**1,749**
101	sp|Q9CPR4|RL17_MOUSE	60S ribosomal protein L17 OS=Mus musculus GN=Rpl17 PE=2 SV=3	0,034	**1,732**
102	sp|P84099|RL19_MOUSE	60S ribosomal protein L19 OS=Mus musculus GN=Rpl19 PE=1 SV=1	0,034	**1,719**
103	sp|Q9CY66|GAR1_MOUSE	H/ACA ribonucleoprotein complex subunit 1 OS=Mus musculus GN=Gar1 PE=2 SV=1	0,034	**1,711**
104	sp|P47963|RL13_MOUSE	60S ribosomal protein L13 OS=Mus musculus GN=Rpl13 PE=2 SV=3	0,034	**1,692**
105	sp|Q9CXW4|RL11_MOUSE	60S ribosomal protein L11 OS=Mus musculus GN=Rpl11 PE=1 SV=4	0,034	**1,616**
27	sp|Q9D6Z1|NOP56_MOUSE	Nucleolar protein 56 OS=Mus musculus GN=Nop56 PE=1 SV=2	0,034	**1,582**
28	sp|P14148|RL7_MOUSE	60S ribosomal protein L7 OS=Mus musculus GN=Rpl7 PE=2 SV=2	0,034	**1,486**
22	sp|Q99MN1|SYK_MOUSE	Lysine--tRNA ligase OS=Mus musculus GN=Kars PE=1 SV=1	0,034	**1,469**
6	sp|Q9D7S7|RL22L_MOUSE	60S ribosomal protein L22-like 1 OS=Mus musculus GN=Rpl22l1 PE=1 SV=1	0,034	**1,469**
7	sp|Q6ZWV7|RL35_MOUSE	60S ribosomal protein L35 OS=Mus musculus GN=Rpl35 PE=2 SV=1	0,034	**1,467**
8	sp|P62855|RS26_MOUSE	40S ribosomal protein S26 OS=Mus musculus GN=Rps26 PE=2 SV=3	0,034	**1,464**
9	sp|Q6ZWX6|IF2A_MOUSE	Eukaryotic translation initiation factor 2 subunit 1 OS=Mus musculus GN=Eif2s1 PE=1	0,034	**1,422**

10	sp|Q8BP67|RL24_MOUSE	60S ribosomal protein L24 OS=Mus musculus GN=Rpl24 PE=2 SV=2	0,034	**1,418**
11	sp|Q9D6S7|RRFM_MOUSE	Ribosome-recycling factor, mitochondrial OS=Mus musculus GN=Mrrf PE=1 SV=1	0,032	**0,744**
12	sp|O54984|ASNA_MOUSE	ATPase Asna1 OS=Mus musculus GN=Asna1 PE=1 SV=2	0,034	**0,718**
13	sp|Q01405|SC23A_MOUSE	Protein transport protein Sec23A OS=Mus musculus GN=Sec23a PE=1 SV=2	0,034	**0,598**
14	sp|Q99L47|F10A1_MOUSE	Hsc70-interacting protein OS=Mus musculus GN=St13 PE=2 SV=1	0,034	**0,593**
15	sp|P48428|TBCA_MOUSE	Tubulin-specific chaperone A OS=Mus musculus GN=Tbca PE=2 SV=3	0,034	**0,577**
16	sp|P10518|HEM2_MOUSE	Delta-aminolevulinic acid dehydratase OS=Mus musculus GN=Alad PE=1 SV=1	0,034	**0,552**
17	sp|Q9DAU1|CNPY3_MOUSE	Protein canopy homolog 3 OS=Mus musculus GN=Cnpy3 PE=1 SV=1	0,032	**0,543**
18	sp|P62751|RL23A_MOUSE	60S ribosomal protein L23a OS=Mus musculus GN=Rpl23a PE=1 SV=1	0,034	**0,542**
19	sp|Q8BGD9|IF4B_MOUSE	Eukaryotic translation initiation factor 4B OS=Mus musculus GN=Eif4b PE=1 SV=1	0,034	**0,533**
41	sp|Q9CY50|SSRA_MOUSE	Translocon-associated protein subunit alpha OS=Mus musculus GN=Ssr1 PE=1 SV=1	0,034	**0,496**
42	sp|Q8K003|TMA7_MOUSE	Translation machinery-associated protein 7 OS=Mus musculus GN=Tma7 PE=2 SV=1	0,034	**0,487**
4	sp|P47955|RLA1_MOUSE	60S acidic ribosomal protein P1 OS=Mus musculus GN=Rplp1 PE=1 SV=1	0,034	**0,470**
5	sp|Q62446|FKBP3_MOUSE	Peptidyl-prolyl cis-trans isomerase FKBP3 OS=Mus musculus GN=Fkbp3 PE=1 SV=2	0,034	**0,467**
6	sp|P62852|RS25_MOUSE	40S ribosomal protein S25 OS=Mus musculus GN=Rps25 PE=2 SV=1	0,034	**0,396**
16	sp|O70251|EF1B_MOUSE	Elongation factor 1-beta OS=Mus musculus GN=Eef1b PE=1 SV=5	0,034	**0,382**
17	sp|Q8BP92|RCN2_MOUSE	Reticulocalbin-2 OS=Mus musculus GN=Rcn2 PE=2 SV=1	0,034	**0,321**
18	sp|Q03958|PFD6_MOUSE	Prefoldin subunit 6 OS=Mus musculus GN=Pfdn6 PE=2 SV=1	0,034	**0,287**
19	sp|Q99PL5|RRBP1_MOUSE	Ribosome-binding protein 1 OS=Mus musculus GN=Rrbp1 PE=2 SV=2	0,034	**0,274**
20	sp|O70591|PFD2_MOUSE	Prefoldin subunit 2 OS=Mus musculus GN=Pfdn2 PE=2 SV=2	0,034	**0,256**
5	sp|P99027|RLA2_MOUSE	60S acidic ribosomal protein P2 OS=Mus musculus GN=Rplp2 PE=1 SV=3	0,034	**0,222**

Transporter- ion channel- receptor

50	sp|Q9ERK4|XPO2_MOUSE	Exportin-2 OS=Mus musculus GN=Cse1l PE=2 SV=1	0,034	**3,182**
93	sp|Q9QYB1|CLIC4_MOUSE	Chloride intracellular channel protein 4 OS=Mus musculus GN=Clic4 PE=1 SV=3	0,034	**1,828**
94	sp|Q8BKC5|IPO5_MOUSE	Importin-5 OS=Mus musculus GN=Ipo5 PE=1 SV=3	0,034	**1,551**
95	sp|Q9EPL8|IPO7_MOUSE	Importin-7 OS=Mus musculus GN=Ipo7 PE=1 SV=2	0,034	**1,448**
39	sp|P55012|S12A2_MOUSE	Solute carrier family 12 member 2 OS=Mus musculus GN=Slc12a2 PE=1 SV=2	0,034	**0,590**

Vescicle metabolism

1	sp|Q9ES97|RTN3_MOUSE	Reticulon-3 OS=Mus musculus GN=Rtn3 PE=1 SV=2	0,034	**1,671**
2	sp|Q9CWZ7|SNAG_MOUSE	Gamma-soluble NSF attachment protein OS=Mus musculus GN=Napg PE=1 SV=1	0,034	**1,611**
3	sp|Q9D8B3|CHM4B_MOUSE	Charged multivesicular body protein 4b OS=Mus musculus GN=Chmp4b PE=2 SV=2	0,034	**0,740**
4	sp|Q9CQ10|CHMP3_MOUSE	Charged multivesicular body protein 3 OS=Mus musculus GN=Chmp3 PE=1 SV=3	0,034	**0,648**
8	sp|P55302|AMRP_MOUSE	Alpha-2-macroglobulin receptor-associated protein OS=Mus musculus GN=Lrpap1 PE=	0,034	**0,619**
9	sp|Q9QY76|VAPB_MOUSE	Vesicle-associated membrane protein-associated protein B OS=Mus musculus GN=Vap	0,034	**0,592**
10	sp|O70439|STX7_MOUSE	Syntaxin-7 OS=Mus musculus GN=Stx7 PE=1 SV=3	0,034	**0,568**
11	sp|Q7TQF7|AMPH_MOUSE	Amphiphysin OS=Mus musculus GN=Amph PE=1 SV=1	0,034	**0,494**
12	sp|O35526|STX1A_MOUSE	Syntaxin-1A OS=Mus musculus GN=Stx1a PE=1 SV=3	0,034	**0,392**
13	sp|O08585|CLCA_MOUSE	Clathrin light chain A OS=Mus musculus GN=Clta PE=1 SV=2	0,034	**0,387**
14	sp|O55042|SYUA_MOUSE	Alpha-synuclein OS=Mus musculus GN=Snca PE=1 SV=2	0,034	**0,322**

rest /unknown

1	sp|Q8K2Q7|BROX_MOUSE	BRO1 domain-containing protein BROX OS=Mus musculus GN=Brox PE=2 SV=1	0,034	**1,726**

2	sp|Q6P8X1|SNX6_MOUSE	Sorting nexin-6 OS=Mus musculus GN=Snx6 PE=1 SV=2	0,032	**1,690**
3	sp|Q99J36|THUM1_MOUSE	THUMP domain-containing protein 1 OS=Mus musculus GN=Thumpd1 PE=1 SV=1	0,032	**0,753**
19	sp|Q6PGH2|HN1L_MOUSE	Hematological and neurological expressed 1-like protein OS=Mus musculus GN=Hn1l P	0,034	**0,714**
20	sp|Q8C8R3|ANK2_MOUSE	Ankyrin-2 OS=Mus musculus GN=Ank2 PE=1 SV=2	0,034	**0,610**
21	sp|Q9D8Y0|EFHD2_MOUSE	EF-hand domain-containing protein D2 OS=Mus musculus GN=Efhd2 PE=1 SV=1	0,034	**0,594**
42	sp|Q9CYZ2|TPD54_MOUSE	Tumor protein D54 OS=Mus musculus GN=Tpd52l2 PE=1 SV=1	0,034	**0,593**
32	sp|Q4VAA2|CDV3_MOUSE	Protein CDV3 OS=Mus musculus GN=Cdv3 PE=1 SV=2	0,034	**0,578**
33	sp|Q9R0P4|SMAP_MOUSE	Small acidic protein OS=Mus musculus GN=Smap PE=1 SV=1	0,034	**0,498**
34	sp|Q3UHX2|HAP28_MOUSE	28 kDa heat- and acid-stable phosphoprotein OS=Mus musculus GN=Pdap1 PE=1 SV=	0,032	**0,468**
35	sp|Q9CQH7|BT3L4_MOUSE	Transcription factor BTF3 homolog 4 OS=Mus musculus GN=Btf3l4 PE=2 SV=1	0,034	**0,442**
36	sp|Q9DCT8|CRIP2_MOUSE	Cysteine-rich protein 2 OS=Mus musculus GN=Crip2 PE=1 SV=1	0,034	**0,440**
37	sp|P31786|ACBP_MOUSE	Acyl-CoA-binding protein OS=Mus musculus GN=Dbi PE=1 SV=2	0,034	**0,357**